

A fluvial record of plate-boundary deformation in the Olympics Mountains

Frank J. Pazzaglia
Department of Earth and Environmental Sciences
Lehigh University
Bethlehem, PA 18015

Mark T. Brandon
Department of Geology and Geophysics
Yale University
New Haven, CT 06520-8109

Karl W. Wegmann
Washington Dept. of Natural Resource
Division of Geology & Earth Resources
Olympia, WA 98504-7007

Trip Overview

We have constructed a 2-day field trip designed to exhibit the geology, geomorphology, and active tectonics of the Pacific coast of the Olympic Peninsula. The trip is organized around the following three major topics that should generate lively discourse on how to use and interpret basic field relationships in tectonic geomorphology research:

- (1) What is a river terrace, how is it made, and what do river terraces tell us about active tectonics?
- (2) What is driving orogenesis for the Olympic Mountain segment of the Cascadia Subduction Zone? Is it shortening parallel to the direction of plate convergence, shortening normal to the direction of plate convergence, or some combination of both? Are there any geomorphic or stratigraphic field relationships that can actually be used to track the horizontal movement of rocks and thus interpret the shortening history over geologic time scales?
- (3) We know that uplift along Cascadia includes the effects of cyclic earthquake-related deformation, and long-term steady deformation. How do these different types of uplift influence incision and aggradation in the rivers of the Olympic Mountains?

The trip begins by building a Quaternary stratigraphic foundation along the western coast of the Olympic Peninsula and then works landward into the Clearwater drainage. As far as possible, we will present the deposits in stratigraphic order, from oldest to youngest. Throughout the trip, we will show the data and reasoning for the spatial correlation of deposits, their numeric age, and the resulting tectonic implications. An important consideration in understanding deformation in this setting is how rocks move horizontally through the subduction wedge. We present geomorphic and stratigraphic data to help resolve the horizontal translation of rocks and thus provide some constraints for shortening over geologic time scales.

Fluvial terraces are the main source of geologic and Quaternary stratigraphic data used in our tectonic interpretations. Terraces are landforms that are underlain by an alluvial deposit, which in turn sit on top of a strath, which is an unconformity of variable lateral extent and local relief. Typically, the strath is carved into bedrock, but it can also be cut into older alluvial deposits. At the coast, we recognize straths and their accompanying overlying alluvial deposits, and then show how those features continue upstream into the Clearwater River drainage. The straths and terraces are exposed because there has been active incision of the river into the rocks of the Olympic Peninsula. The most obvious conclusion is that river incision is a response to active rock uplift. But straths and terraces indicate that the incision history of at least one river has not been perfectly steady. There has been variability in external factors, such as climate or tectonics, which have modulated the terrace formation process. What we hope to demonstrate is that the variability in incision process and rate is primarily attributed to climate, but that continued uplift provides the means for long-term net incision of the river into the Olympic landscape.

The first day will be mostly dedicated to understanding the coastal stratigraphy in and around Kalaloch where many of our age constraints are located. The field relationships for permanent shortening of the Olympic wedge will also be explored. The second day will be devoted to the Clearwater drainage and an investigation of terraces of various size, genesis, and tectonic implication. We will consider the myriad of processes that have conspired to construct and preserve the terraces and the possible contributions of both cyclic and steady uplift.

Introduction

This field trip is about the use of Quaternary stratigraphy to measure tectonic deformation of the Olympic Mountains section of the Pacific Northwest Coast Range. An important motivation for understanding orogenesis here, and throughout the Coast Range, is the concern about the relationship of active deformation to seismic hazards associated with the Cascadia Subduction Zone. There is also any interest in sorting the nature of the deformation, whether cyclic or permanent, and whether it involves mainly shortening parallel or perpendicular to the margin. Of particular interest is evidence of cyclic deformation related to large earthquakes at or adjacent to the subduction zone (Savage et al., 1981, 1991; Thatcher and Rundle, 1984; Dragert, 1987; Rogers, 1988; Atwater, 1987, 1996; Holdahl et al., 1987, 1989; West and McCrumb, 1988; Darenzio and Peterson, 1990; Atwater et al., 1991; Bucknam et al., 1992; Hyndman and Wang, 1993; Dragert et al., 1994; Mitchell et al., 1994). Fundamental to these studies is the distinction between short-term ($10^2 - 10^3$ yr) cyclic elastic deformation adjacent to the seismogenic subduction thrust and long-term ($10^4 - 10^5$ yr) permanent deformation associated with growth and deformation of the overlying Cascadia wedge. Holocene deposits preserved in locally subsiding estuaries along the west coast of the Olympics provide good evidence of cyclic deformation related to large prehistoric earthquakes (Atwater, 1987, 1996). Seismogenic slip associated with these earthquakes, both on the subduction thrust and also on upper-plate faults, contributes to long-term deformation of the margin. However, it is difficult to separate elastic deformation, which is created and then recovered during each earthquake cycle, from the permanent deformation associated with fault slip. The earthquake cycle is probably partly decoupled from the permanent deformation, so we cannot easily integrate the effects of numerous earthquake cycles and arrive at the final long-term deformation. Furthermore,

aseismic ductile flow, occurring within the deeper parts of the Cascadia wedge, probably also contributes to deformation manifest over long time spans.

Pre-Holocene stratigraphy and structure provide the only records of sufficient duration to separate long-term permanent deformation from earthquake-cycle elastic deformation. For this reason, local active-tectonic studies have focused on deformation of Quaternary deposits and landforms, which are best preserved along the Pacific Coast and offshore on the continental shelf (Rau, 1973, 1975, 1979; Adams, 1984; West and McCrumb, 1988; Kelsey, 1990; Bockheim et al., 1992; Kelsey and Bockheim, 1994; Thackray and Pazzaglia, 1994; McCrory, 1996, 1997; McNeill et al., 1997; Thackray, 1998; McNeill et al., 2000). Mud diapirism, which is widespread beneath the continental shelf and along the west coast of the Olympics (Rau and Grocock, 1974; Rau, 1975; Orange, 1990), may be a local factor contributing to the observed deformation of Quaternary deposits.

In contrast, much less is known about the long-term deformation of the coastal mountains that flank the Cascadia margin (Figure 1). The development and maintenance of the Oregon-Washington Coast Range as a topographic high suggests that it is an actively deforming part of the Cascadia plate boundary. Diverse geologic and geodetic datasets seem to indicate shortening and uplift both parallel (Wang, 1996; Wells et al., 1998) and normal (Brandon and Calderwood, 1990; Brandon and Vance, 1992; Brandon et al., 1998) to the direction of convergence (Figure 2). This relationship is best documented in the Olympic Mountains (Figures 1b,c), which, on a geologic time scale ($> 10^3$ yr), seems to be the fastest deforming part of the Cascadia forearc high. The Olympic Mountains occupy a 5800 km² area within the Olympic Peninsula. The central part of the range has an average elevation of ~1200 m, and reaches a maximum of 2417 m at Mount Olympus (Figure 1c). The Olympics first emerged above sea level at ~18 Ma (Brandon and Vance, 1992), and they then seem to have quickly evolved into a steady-state mountain range, defined here by rock uplift rates that are closely balanced by erosion rates (Brandon et al., 1998). Fission-track-cooling ages indicate that the fastest erosion rates, ~0.8 m/k.y., are localized over the highest part of the range (Figure 2). Rocks exposed there were deposited and accreted in the Cascadia trench during the late Oligocene and early Miocene, and then exhumed from a depth of ~12 - 14 km over the past 16 m.y. Present-day rugged relief and high-standing topography are consistent with ongoing tectonic activity.

Geodetic and tide-gauge data (Reilinger and Adams, 1982; Holdahl et al., 1989; Savage et al., 1991; Mitchell et al., 1994) indicate that short-term uplift is very fast on the Olympic Peninsula, ranging from 1.2 to 3.2 m/k.y., with the highest rates along the west side of the peninsula (Figure 2). These large rates probably include a significant component of earthquake-cycle elastic deformation, given that the Cascadia Subduction thrust is presently locked. This conclusion is supported by geologic evidence that indicates insignificant long-term uplift or growth in coastal regions around the peninsula over the past 10 m.y. For instance, exposures of upper Miocene to lower Pliocene shallow-marine deposits locally crop out near modern sea level (e.g., Montesano and Quinault formations; see Tq in Figure 2) (Rau, 1970; Tabor and Cady, 1978a; Armentrout, 1981; Bigelow, 1987; Palmer and Lingley, 1989; Campbell and Nesbitt, 2000). These units currently sit within ~200 m of their original depositional elevation, which implies rock-uplift rates less than about 0.05 m/k.y. Slow long-term rock and surface uplift is also consistent with

the preservation of extensive middle and lower Pleistocene deposits and constructional landforms along much of the west coast (Thackray and Pazzaglia, 1994; Thackray, 1998).

Our objective here is to use fluvial terraces to examine the pattern and rates of long-term river incision across the transition from the relatively stable Pacific coast to the actively uplifting interior of the Olympic Mountains. We have focused on the Clearwater drainage (Figure 1b; Figure 3), which remained unglaciated during the late Pleistocene and Holocene, and thus was able to preserve a flight of fluvial terraces, with each terrace recording the shape and height of past long profiles, with the oldest record extending back into the middle Pleistocene. An important advantage of the Clearwater River is that its main channel has an orientation roughly parallel to the Juan de Fuca – North America convergence direction, and thus it is well-situated to document shortening normal to the margin. We assess how fluvial terraces are formed in this setting and then use features of the terraces to estimate incision rates along the Clearwater long profile. Geologic relationships and geodetic data are used to examine the degree of horizontal shortening in the direction of plate convergence for the Cascadia forearc high. The long fluvial history preserved in the Clearwater ensures that the unsteady deformation associated with the earthquake cycle is averaged out, leaving us with a record of long-term uplift. We show, however, that the earthquake cycle may play an important role in terrace genesis at the millennial time scale.

Tectonic Setting

The Cascadia subduction zone underlies a doubly vergent wedge (in the sense of Koons, 1990, and Willett et al., 1993). The change in vergence occurs at the crest of the Oregon-Washington Coast Range, which represents the forearc high. The doubly vergent system includes a prowedge (or proside) that overrides oceanic lithosphere and accretes turbidites of the Cascadia drainage, and a retrowedge (or retroside) that underlies the east-facing flank of the Coast Range (Willett, 1999; Beaumont et al., 1999) (Figure 4). This usage emphasizes the asymmetry of the underlying subduction zone, defined by subduction of the pro-plate (Juan de Fuca) beneath the retro-plate (North America).

Much of the Cascadia forearc high is underlain by the Coast Range Terrane, a slab of lower Eocene oceanic crust (Crescent Formation and Siletz River Volcanics), which occurs as a landward-dipping unit within the Cascadia wedge (Figure 1a) (Clowes et al., 1987). Accreted sediment that makes up the proside of the wedge reaches a thickness of 15-25 km at the present Pacific Coast (Figures 1 and 4) and locally extends landward beneath the Coast Range Terrane. The Coast Range Terrane is clearly involved in subduction-related deformation, even though the rate of deformation is relatively slow when compared with the accretionary deformation occurring at the toe of the seaward wedge. Nonetheless, the Cascadia wedge, by definition, includes all rocks that are actively deforming above the Cascadia Subduction Zone. Thus, the Coast Range Terrane cannot be considered a rigid "backstop", but instead represents a fully involved component of the wedge.

In the Olympic Mountains, the Coast Range Terrane has been uplifted and eroded away, exposing the Hurricane Ridge Thrust and the underlying Olympic Subduction Complex (OSC) (Figures 1 and 3). The OSC is dominated by relatively competent and homogeneous assemblage

of sandstone and mudstone, with minor conglomerate, siltstone, and basalt (Tabor and Cady, 1978a, b). A large part of the OSC was formed by accretion of seafloor turbidites into the proside of the wedge, starting at about 35 Ma (Brandon et al., 1998). Where exposed in the Olympics, those accreted sediments are now hard well-lithified rocks. The steep rugged topography of the Olympics is supported by both basalts of the Coast Range Terrane and accreted sediment of the OSC, which suggests that there is little difference in their frictional strength. Uplift in the Olympic Mountains has been driven by both accretion and within-wedge deformation (Figure 4) (Brandon and Vance, 1992; Willett et al. 1993, see stage 2 of their Figure 2; Brandon et al., 1998). Accretion occurs entirely on the proside of the wedge, resulting in decreasing material velocities toward the rear of the wedge. In the Olympics, retroside deformation is marked by folding of the Coast Range Terrane into a large eastward-vergent structure (Tabor and Cady, 1978a,b). The upper limb of that fold, which underlies the eastern flank of the Olympics (Figure 4), is steep and locally overturned, in a fashion similar to the folding illustrated in Willett et al. (1993, stage 2 in their Figure 2). We infer from the steep topographic slope on the retroside of the wedge that folding is being driven by a flux of material from the proside of the wedge, and that the wedge has not yet begun to advance over the retroside plate (Willett et al., 1993).

Deep erosion and high topography in the Olympics are attributed to an arch in the subducting Juan de Fuca Plate (Brandon and Calderwood, 1990; Brandon et al., 1998). The subducting plate is about 10 km shallower beneath the Olympics relative to areas along strike in southwest Washington and southern Vancouver Island (Crossen and Owens, 1987; Brandon and Calderwood, 1990). Stated in another way, the shallow slab beneath the Olympics means that less accommodation space is available to hold the growing Cascadia wedge (Brandon et al., 1998). This situation, plus higher convergence rates and thicker trench fill along the northern Cascadia Trench, has caused the Olympics to become the first part of the Cascadia forearc high to rise above sea level. The early development of subaerial topography, plus continued accretion and uplift, account for the deep erosion observed in the Olympics. The corollary to this interpretation is that adjacent parts of the forearc high will evolve in the same way, although more slowly because of lower accretionary fluxes and a larger accommodation space for the growing wedge.

Field Results

DAY 1. Coastal exposures near Kalaloch, Olympic National Park, Moses Prairie paleo sea cliff, model terrace in the Clearwater drainage (Figure 5).

Miles	Description
0.0	START, Kalaloch Lodge. Walk to the beach overlook for a brief overview. Kalaloch and the entire field-trip route lie in the west central part of the Olympic Peninsula, between two large drainages, the Hoh and Queets rivers that drain the northwest, west, and southwest flank of Mt. Olympus (Figures 1b, 3a). The Clearwater River is tucked away between these two master drainages, and we use the fluvial and glacial deposits of the Hoh and Queets rivers to constrain the ages of terraces in the Clearwater drainage (Figure 6). The Olympic coast here is a constructional feature underlain by glaciofluvial deposits. It lacks the distinct,

uplifted marine terraces characteristic of Cascadia in Oregon and northern California, although the effects of glacio-eustasy and coastal tectonics cause a major unconformity in the coastal stratigraphy. Both stratigraphy and correlation of the widespread unconformity indicate active tectonic deformation in the form of a broad (10s of km) fold with an axis oriented roughly northeast or parallel to the direction of convergence (Rau, 1973; McCrory, 1996; Thackray, 1998). The mouth of the Queets River marks the approximate southern limb of a syncline centered on Kalaloch, and the mouth of the Hoh River marks the northern limb of the syncline. The significance of this syncline and all associated broad folding of Quaternary deposits at the coast is in the general lack of significant rock uplift and the comparatively small amount of northerly shortening in comparison to the large amount of shortening and uplift in the direction of plate convergence. The relative tectonic stability of the coast is also supported by preservation of early Pleistocene glaciofluvial deposits, as well as Miocene-Pliocene neritic shelf-basin deposits like the Quinault and Montesano Formation that outcrop at or near sea level. However the precise paleoelevation history of such ancient deposits, like the Quinault and Montesano formations, must be viewed in the context of the large but unknown degree of horizontal translation they have experienced because of wedge shortening.

The tectonic story that we begin weaving here has the following three major themes:

- (1) deformation that is linked to the real-time measurable effects of elastic-strain accumulation and release during the subduction-earthquake cycle (Figure 2a)
- (2) deformation linked to the long-term pattern of rock exhumation revealed by thermochronology (Figure 2a), and
- (3) deformation linked to suggested northward translation of the Coast Range Terrane (Figure 2b).

Our data are well suited to evaluating the geomorphic expression of points (1) and (2), and we will try to illustrate how these are likely to predominate over point (3) in orogenesis in the Olympic Mountains.

- 0.5 National Park Service Kalaloch campground to your left. Highway 101 hugs the coast, traveling on a tread about 20 m in elevation. This tread is underlain by late Pleistocene alluvial and eolian deposits as well as Holocene marsh deposits.
- 2.5 Pass Brown's Point (Beach Trail 3) and rise onto a 30-m terrace tread. This 30-m terrace is well preserved along the coast and will figure significantly into the stratigraphic story.
- 3.3 **STOP 1-1. Beach Trail 4.** The purpose of this stop will be to see the rocks of the Cascadia wedge and begin developing the stratigraphic framework of the

Quaternary deposits by observing the 122 ka wave-cut unconformity. A key point is that rocks exposed at the coast may have moved northeastward into the coast, with little to no uplift. Park in the NPS parking lot and descend the trail leaving from the southeast corner of the lot and go to beach level.

The bedrock exposed here consists of turbidites of the Miocene Hoh Formation (Figure 7a). These rocks were deposited on the continental slope in at least 2 km of water and have been uplifted here to sea level. More importantly, the Hoh Formation was laid down 50 to 100 km west of its current position and has since followed a largely horizontal trajectory to the present Olympic coastline (Figure 4). The nearly vertically bedded bedrock is planed off at approximately 2.7 m above mean sea level by a wave-cut unconformity. A thin boulder lag locally lies atop the unconformity, and it is superceded by gray pebbly beach sand texturally and structurally identical to the modern exposed shoreface. Exposures along the trail leading to the beach clearly show the unconformity continuing west under the 30 m coastal terrace (Figure 8). Cylindrical borings in the Hoh beneath the unconformity are interpreted as being shaped in part by pholad clams. The stratified sand, gravel, and peat overlying the beach deposits are part of the Browns Point Formation (Huesser, 1972; Figure 7b). Gravel clasts in this deposit tend to be weathered and their provenance is consistent with a local source, most likely Kalaloch ridge directly to the west, rather than the Hoh or Queets rivers, whose deposits tend to be less weathered. The Browns Point Formation seems to represent a long period of fluvial, glacio-fluvial, and marsh-type sedimentation. The base of the unit directly above the beach sands is radiocarbon dead, but stratigraphically higher deposit have a progressively younging sequence of radiocarbon ages (Huesser, 1972; Thackray, 1996). The youngest age comes from about 6 m below the terrace tread and is $16,700 \pm 160$ radiocarbon years before present.

The wave-cut unconformity here (Figure 7a) is a key stratigraphic horizon that can be traced for 80 km along the coast. It does not remain at the elevation viewed here. At Kalaloch, the unconformity is below sea level and not exposed. And it rises to a maximum of 52 m above sea level south of the mouth of the Queets River. The average elevation between the mouth of the Hoh and Queets rivers is 11 meters. Deposits both above and below the unconformity are radiocarbon dead. We propose at this stop, and then will develop the evidence at subsequent stops, that the unconformity represents a wave-cut surface, produced during eastward migration of a shoreface during the last major interglacial eustatic highstand, at 122 ka (isotope stage 5e).

5.3 Cross Steamboat Creek and slow for a left turn.

5.4 **Turn left. STOP 1-2. Beach Trail 6.** The purpose of this stop will be to observe the Quaternary deposits above and below the wave-cut unconformity, as well as key points for numeric ages of the deposits. We follow the field observation of these units with a map-based correlation to glacial deposits in the

Hoh and Queets river valleys. Park in the National Park Service lot and access the trail that heads into the woods on the northwest corner of the lot. The exposures at Beach Trail 6 have changed significantly in recent years because of landsliding and coastal erosion. The trail is difficult to follow in places, and we urge care in descending the sea cliff. The deposits underlying the 30-m terrace are well exposed in the landslide headscarp. In particular, a 1-2 m cap of loess, with a yellowish-brown soil developed in it, can be seen conformably overlying stratified sand and gravel.

The wave-cut unconformity is higher here, at about 12 m above sea level, and is marked by a boulder lag (Figure 9). The deposit below the unconformity was first named and described by Florer (1972) as the Steamboat Springs Formation. It is a complexly interbedded sequence of till, lacustrine deposits, glaciofluvial outwash, and sand dunes, which has yielded only infinite radiocarbon ages (below the detection limit for radiocarbon). Samples collected from lacustrine beds within this unit by Pazzaglia and Thackray, and analyzed by H. Rowe and J. Geissman at the University of New Mexico, show both normal and reversed polarities (Thackray, 1996). At this site in particular, the polarity of the sample is reversed indicating an age greater than 780 ka, the most recent reversal. Beach deposits overlie the unconformity and are succeeded by predominantly glaciofluvial outwash sourced from the Hoh drainage. The outwash within 15 m of the unconformity is interbedded locally with peaty beds that have returned radiocarbon-dead ages of >33.7 and >48 ka (Florer, 1972). Closer to the terrace tread, typically within 5 m of the surface, finite radiocarbon ages of $36,760 \pm 840$, $28,352 \pm 504$, and $24,422$ radiocarbon years before present have been dated on woody material by Thackray (1996). The interpretation of these ages suggested by Thackray (1996, 2001) is that the outwash directly above the wave-cut unconformity is correlative to a marine isotope stage 4 (or possibly 5d,b) alpine glaciation and that the finite radiocarbon ages near the top of the section is sourced from outwash draining isotope stage 2 or 3 alpine glaciers. A difficult to discern gravel-on-gravel unconformity between isotope stage 4 and isotope stage 2 or 3 deposits is implied by this interpretation.

The new landslides here at Beach Trail 6 expose mud diapirs that are both overlapped by and pierce the Steamboat Springs Formation (Rau and Grocock, 1974; Rau, 1975; Orange, 1990).

Return to the parking lot and assemble at the overlook of the coast and Destruction Island. The broad topographic and structural low between the mouth of the Hoh and Queets rivers filled with sediment from those two point sources, as well as from small streams draining Kalaloch Ridge (Figure 8). The center of the low near Kalaloch has more fine-grained sediment than the regions proximal to the big river mouths. The general model is that the Queets and Hoh Rivers have periodically been point sources that built broad fans in front of the river mouths, spilling laterally into the Kalaloch low. The fans formerly extended far west of the current coast. The top of Destruction Island 5 km offshore (20 m elevation) is

correlative to the 30-m tread here at the coast, and the flanged base of Destruction Island that sits only 1 m above mean tide level is the westward continuation of the wave-cut unconformity. The level of the fan tread, represented by the 30-m terrace we have been traveling on all morning, must reflect a significant amount of vertical aggradation rather than tectonic uplift. The preservation of the isotope stage 5e unconformity and approximately 800 ka Pleistocene deposits attest to the relative tectonic stability of the coast.

The most likely time for major periods of fan aggradation on a generally tectonically stable coastal setting is during a cycle of alpine deglaciation, as the river valleys are liberating a high sediment flux at the same time sea level is rising. It is difficult to imagine how the observed degree of aggradation could have occurred during relative sea level low on a coast not undergoing rapid vertical uplift. Furthermore, map relationships show how the coastal terrace treads can be traced more or less continuously up the Hoh and Queets valleys to heads of outwash (moraines). The general glacial stratigraphy of the Hoh and Queets valleys (Thackray, 1996; 2001; Figure 6) records a major isotope stage 4 alpine glaciation (60 ka, Lyman Rapids drift) that was responsible for the large body of outwash above the wave-cut unconformity and the construction of the 30-m terrace at the coast. Older alpine glacial periods, such as isotope 6 (150 ka, Whale Creek drift), are represented by the deposits below the wave-cut unconformity. However, there are clearly deposits older than isotope stage 6 below the unconformity, and these have a landward equivalent in various upland gravels locally called the Wolf Creek drift. Deposits of isotope stage 3 and 2 alpine glacial periods are underrepresented at the coast because of the relative small size of the glaciations.

Our next stop will further develop the correlation between the glacial and fluvial record in the river drainages to the stratigraphy at the coast by focusing on the remnants of the sea cliff present during the cutting of the isotope stage 5e wave-cut unconformity.

Return to vehicles, exit parking lot, and turn right (south) onto U.S. Route 101.

- 10.3 Turn Right into the Kalaloch campground. This is the **LUNCH** stop. Return to Rt. 101 south following lunch.
- 10.8 Pass Kalaloch Lodge.
- 13.5 South Beach campground is to the right. The 20-m tread here has been dated as 4570 ± 60 radio carbon years before present. The dated material unconformably overlies late Pleistocene alluvium.
- 15.7 Cross the Queets River. Highway 101 is following a big meander loop of the Queets River. To your left are several late Pleistocene to Holocene terraces and sloughs. To the right are treads of the 30-m terrace. Engineering borings for the

bridge show that the alluvium is thin (6 m); there is no deep, filled thalweg beneath the river channel. In other words, the river is essentially running over a low-relief bedrock strath.

- 18.4 Turn right and stay straight on the dirt road. You are now on Quinault Nation land, and you need access permission from the tribal government in Tahola. Moses Prairie is to your left, following the valley of the North Fork Whale Creek.
- 19.2 Stay left on the main dirt road, cross the North Fork Whale Creek and begin to ascend the 60-m terrace.
- 19.9 Proceed to the fork in the road and turn around. This is **STOP 1-3. Moses Prairie**. The objective is to observe the paleo sea cliff, relate the 30-m and 60-m coastal treads to glaciations in the Hoh and Queets River valleys, and discuss how the paleo sea cliff tracks the horizontal motion of rocks and shortening of the wedge. The road from this stop crosses Moses Prairie, a site of active marsh deposition along the North Fork Whale Creek, slightly inset into the 30-m tread. Pazzaglia, Thackray, and W. Gerstel extracted a hand-augered core from this bog in 1994. The core extended down 10 m until refusal in pebbly sandy silt. The point of refusal is taken to be the contact between the Moses Prairie / North Fork Whale Creek marsh/alluvial deposits and the isotope stage 4 glaciofluvial deposits of the 30-m terrace. Two radiocarbon determinations from the base of the core returned ages of $33,182 \pm 756$ and $36,256 \pm 807$ radiocarbon years before present (Thackray, 1996; 2001). These ages are consistent with the idea that the glaciofluvial outwash underlying the bulk of the 30-m terrace is radiocarbon dead but younger than the wave-cut unconformity, leading to its isotope stage 4 (60 ka) age assignment.

Our stop here is on a terrace tread 60 meters in elevation, which looks out over the 30-m tread that we have been traveling on all morning (Figure 9). Like the 30-m terrace, the 60-m terrace tread is also underlain by alluvial and eolian deposits; however, they tend to be much more deeply weathered, to exhibit reddish soil colors, and to locally contain saprolitized gravel clasts. The terrace riser between the 30-m and 60-m terrace parallels the modern sea cliff and Queets River valley margin. We propose that the 60-m terrace represents an older, constructional top of a major aggradational fan to alluvial plain that headed in the Queets valley well before deposition of the isotope stage 4 deposits underlying the 30-m terrace. This older aggradational alluvial plain would have once extended far west of its current location. But in the same way that relatively high Holocene sea level is driving an eastward retreat of the coastal sea cliff into the 30-m terrace, the high relative sea level of the last major interglaciation, during isotope stage 5e, drove eastward retreat of a former seacliff into the older deposits underlying the 60-m terrace. Continuing with this logic, the eastward retreat of this paleo sea cliff would be synonymous with the cutting of the wave-cut unconformity. So the idea suggested at Stop 1-2, that the glaciofluvial deposits beneath the wave-cut unconformity is attributed to a isotope stage 6 (or older)

alpine glacial outwash event, is strongly supported by finding remnants of the older alluvial deposits truncated by the paleosea cliff. Coastal aggradation during the isotope stage 4 alpine glacial event buried the isotope stage 5e beach deposits and subsequently filled-in the area in front of the paleo sea cliff. We envision, and locally observe, a distinct buttress unconformity between the 30 m terrace tread of Moses Prairie and the terrace riser of the 60-m terrace.

The location of the paleo sea cliff with respect to the modern sea cliff contains information about how rocks are surfing horizontally through the Olympic wedge. In general, rocks at the Earth's surface move in both vertical and horizontal directions (Willett et al., 2001). Based on the apparent rapid retreat of the modern coastline during the Holocene (as discussed at the last stop), it would seem that a retreating sea cliff is able to rapidly adjust to rising sea level. Thus, we assume that the horizontal distance between the paleo sea cliff and the modern sea cliff is due solely to eustasy and tectonic displacement (Figure 10).

We used Bruun's rule (Dean, 1991) to estimate how much the modern sea cliff would be translated landward if modern sea level were to rise to the height of the 122 ka Sangamon highstand. According to this relationship, a rise in sea level S would cause a landward shift (Δx) in the shoreline of

$$\Delta x = S w_w / (h_w + h_b), \quad (1)$$

where w_w and h_w are the width and maximum depth of the breaker zone, and h_b is the berm height on the beach. A 17 year-record for a deep-water (2780 m) buoy offshore of the Queets River indicates that waves coming into that coastline have maximum heights of 13.6 m and maximum periods of 18 seconds in the open ocean (buoy 46005, National Data Buoy Center, 2000). Using relationships in Trenhaile (1997, see his p. 22), those waves indicate a maximum breaker depth $h_w = 14.0 \pm 1.0$ m (uncertainties are ± 1 SE). The nearshore profile indicates that this depth lies offshore at $w_w = 2850 \pm 220$ m. The berm height h_b is about 1 m. Bruun's rule indicates that if modern sea level were to rise to the Sangamon highstand ($S = +5 \pm 0.7$ m), the Sangamon sea cliff should have formed 945 ± 145 m inland with respect to the modern sea cliff. The sea cliff presently lies 505 ± 150 m farther inland, a difference that we attribute to tectonic displacement (Figure 10).

Tectonic displacement of the sea cliff is assumed to have occurred parallel to the convergence direction, which is 26 degrees counterclockwise from perpendicular to the coast line. The cross section in Figure 10 was constructed along the convergence direction at the mouth of the Queets River, and it shows both the horizontal and vertical components of the displacement, along with the predicted eustatic and tectonic components of those displacements. The predicted horizontal tectonic displacement is 450 ± 135 m, accomplished over 122 ± 2 ka, which gives a long-term horizontal tectonic velocity of 3.7 ± 1.1 m/k.y. relative to the adjusted highstand shoreline.

Our interpretation of this result relies on the assumption that the Olympics are in a long-term steady state, meaning that the range is not changing in size with time. This steady-state configuration implies that the shoreline is also in steady state. More specifically, we are assuming that the shoreline returns to the same location at each highstand. Of course, in practice, one would have to correct for small differences in the height of successive highstands (as we have done above). The overall implication is that when the shoreline is at steady state, erosion in the breaker zone is balanced by uplift at the coast. In this case, the calculated tectonic displacement of the paleo sea cliff would represent the horizontal velocity of rocks at the coast relative to the long-term steady-state position of the shoreline. An alternative interpretation is that the Olympics are not in steady state, and the shoreline is moving westward as the mountain range increases in size and width. The coastal geomorphology does not provide any information to distinguish between these two end-member interpretations. However, Pazzaglia and Brandon (2001) do show that frontal accretion into a steady-state Olympics wedge will produce horizontal surface velocities at the coast of 3 m/k.y. Thus, the sea cliff observations are consistent with a steady-state wedge interpretation.

Return to vehicles, and retrace the route back out to Highway 101.

- 21.4 Turn right on Highway 101 and continue on the 30-m tread.
- 24.0 Turn left on the Clearwater-Snahapish Road.
- 24.6 Cross the Queets River. The confluence of the Queets and Clearwater is ahead and to the left. Continue along the Clearwater River. As at the Highway 101 bridge, the engineering borings here demonstrate how the alluvium is thin and stream is essentially on bedrock. The road is on a Holocene (Qt6) terrace. Older Holocene (Qt5) treads are exposed in clearcuts to the right and the treads of the two big Pleistocene fill terraces (Qt2 and Qt3) underlie the hills directly ahead.
- 27.9 Begin ascent of the Qt3 terrace.
- 28.4 To your left and down the bank is a 30-m high landslide headwall exposure of Qt3 gravels unconformably overlying lacustrine beds. The lacustrine beds have been dated at > 47,000 radiocarbon years before present and are likely correlative to Qt2. The overlying Qt3 alluvium has been dated at $48,300 \pm 3,300$ radiocarbon years before present.
- 29.9 Rise onto a degraded tread of Qt2 ~20 m above the Qt3 tread.
- 31.5 Cross Elkhorn Creek incised into the alluvium of Qt3. Stay straight on the paved, main road.

- 32.4 Cross Shale Creek. Note the Qtz alluvium exposed in the creek banks to your right. Such windows into the terrace alluvium, in a direction normal to the main valley, help with reconstructing the 3-D shape of the terrace deposits.
- 32.5 Stay left on the paved main road.
- 33.4 Slow and pull off the road to your left in the parking area just before the bridge. The outcrop is a short walk down the dirt road leading to the river. **STOP 1-4. Holocene strath at the Grouse Bridge.** The purpose of this stop is to introduce the concept of a strath, the terrace deposit, and some of the relative and numeric criteria in establishing strath age. Terraces are well preserved in the Clearwater drainage. There are two major flights of terraces: a higher, outer, older sequence that is underlain by thick alluvial-fill deposits, and a lower, inner, younger sequence underlain by thin alluvial deposits (Figure 11). The terrace exposed here at the Grouse Bridge is a fine example of the lower, inner, younger sequence, and it contains all of the stratigraphic characteristics important to distinguishing and using terraces in tectonic interpretations (Figure 12). The lower terraces like the one exposed here are composed of a basal, coarse grained, 1 to 3 m thick axial channel sandy gravel facies, and overlying fine grained 1-3 m thick sandy silt overbank facies. The sandy gravel facies locally preserves sedimentary structures consistent with lateral accretion processes, as might be expected for point and transverse bars, which we can see in the adjacent modern channel. So by analogy, we take the coarse-grained facies of the terrace deposit to represent the bedload being transported when the terrace strath was cut. In contrast, the fine grained facies represents vertical accretion atop the floodplain, presumably related to deposition during floods.

In an active tectonic setting, the evolution of fluvial processes is both a direct consequence of and an interaction with rock uplift (Bull and Knuepfer, 1987; Wells et al, 1988; Merritts et al., 1994; Personius 1995; Gardner et al., 1992; Burbank et al., 1996; Maddy, 1997; Pazzaglia et al., 1998; Hancock et al., 1999). A important issue during the more than three decades of intense study of fluvial systems in tectonically active settings is how tectonic processes can be isolated from the myriad of geomorphic processes that also influence the genesis and subsequent preservation of fluvial stratigraphy (Schumm, 1969; Schumm et al., 1987; Bull, 1990; Bull, 1991; Sugai, 1993; Tucker and Slingerland, 1997). For example, rapid rates of rock uplift and changes in base level are expected in association with both coseismic and interseismic deformation. These factors introduce the potential for rivers to incise and abandon their valley bottoms as they seek a new base level of erosion (Bull, 1991). But the precise manner in which the rivers accomplish that incision and the nature of the terrace record left behind seems to be dominated by how the drainage responds to changes in climate, most notably, glacial-interglacial-scale climate change (Bull, 1991). Because the dramatic changes in climate tend to occur more frequently than secular changes in the rate of rock uplift, actively incising rivers have the potential to leave a relatively high-resolution record of their incision. The rate of

fluvial incision is commonly interpreted in terms of the rate of rock uplift with the built-in assumption that terrace formation is a short-term disequilibrium phenomena, oscillating about a long-term equilibrium profile more or less represented by the physical characteristics of the modern profile (Knox, 1975; Burbank et al., 1996; Pazzaglia and Brandon, 2001).

River terraces are the geomorphologic and sedimentologic expression of form and process adjustments in a fluvial system (Schumm et al., 1987). Terraces are unconsolidated, allostratigraphic units with a basal unconformity, typically cut across bedrock called a strath, and a constructional bench-like top, called a tread. The terrace deposit between the strath and tread varies in texture, stratification, and thickness. When it is thin (less than 3 m), it represents essentially all of the sediment in transport by a bedrock or mixed bedrock-alluvial channel during bankfull or flood discharges (Wolman and Miller, 1960). In contrast, thicker terrace deposits represent alluvial valley fills, which lift the channel off the strath for some period of time (Bull, 1991). Geologically speaking, the cutting of a strath and deposition of an overlying strath terrace gravel occur at the same time because the moving bedload is what abrades the strath. On the other hand, a fill terrace deposit may take some 100 yr to 10 k.y. to accumulate (Weldon, 1986). Thus, the fill provides only a minimum age for burial of the underlying strath surface.

The process of carving a strath, although not well understood, can be readily observed for many bedrock and mixed bedrock-alluvial channels (Figure 13). In these settings, the width of the valley bottom roughly corresponds to the limits of lateral channel corrasion. Alluvium underlying the floodplain typically is not thicker than 3 m, and during low-flow conditions, bedrock exposed in the channel bottom can be observed to project laterally at the base of the floodplain. Tributary streams that have incised through the floodplain provide additional evidence that the bedrock exposed in the active channel continues laterally as an unconformity at the base of the valley fill. In this respect, the strath beneath a terrace deposit represents the bedrock base of a paleovalley floor and the terrace tread is the constructional top of a paleofloodplain.

Strath terraces are common and typically unpaired in tectonically active areas (Bull, 1991), but they may extend for many kilometers along the length of a valley. It has become clear from diverse tectonically active settings that even though terraces may lie at variable distances above the modern valley bottom, their ages tend to cluster around dates temporally coincident with known climatic changes (Bull and Knuepfer, 1987; Merritts et al., 1994; Burbank et al., 1996; Pazzaglia et al., 1998). Geomorphologists have long recognized this temporal correspondence between terrace age and documented climatic changes and commonly take this as evidence that climate was forcing the change that resulted in strath formation, terrace deposition, and the ultimate preservation of straths and fills (Schumm, 1969; Bull and Knuepfer, 1987; Bull, 1991; Pazzaglia and Gardner, 1993; Meyer et al., 1995; Pazzaglia and Brandon, 2001; Figure 13).

In the Clearwater drainage, we have carefully mapped strath terraces at a 1:12,000 scale (Wegmann, 1999; Pazzaglia and Brandon, 2001). The mapping was carried out both on foot and by traversing the river numerous times in a canoe. Field mapping by canoe was particularly valuable in identifying terrace exposures and finding datable material. The separation between the terrace strath and valley bottom strath was measured directly in the field with a tape measure, accurate to ± 0.01 m for terrace straths less than 10 m above the channel or with an altimeter, accurate to ± 1 m for terrace straths greater than 10 m above the channel. The minimum ages of the straths are estimated by 38 radiocarbon dates (35 AMS and 3 standard beta decay ages) of organic material preserved in the overlying terrace alluvium. On one hand, the similarities between the thin alluvial mantle (< 3 m) above the strath of the modern valley bottom and atop the terrace straths leads us to believe that the cutting of the strath and deposition of the alluvial mantle are essentially contemporaneous processes for strath terraces (Merritts et al., 1994). On the other hand, woody material collected from bars in the active channel have been shown to return radiocarbon ages ranging from modern to over 1000 years (Abbe and Montgomery, 1996a,b). Multiple ages from a single terrace deposit, both at a given locality as well as along the lateral extent of a mapped terrace, helps us access the uncertainty in the age of the fill sequence. We also use these data below to argue for the likelihood of contemporaneous strath cutting and alluvium deposition.

Return to vehicles and retrace the route out to Highway 101 and then up to Kalaloch.

Day 2. Clearwater drainage, terrace stratigraphy, age of Pleistocene terraces, a model for Holocene terrace genesis (Figure 7).

- 0.0 **START** – Grouse Bridge in Clearwater drainage.
- 0.7 Cross the Clearwater River and ascend the Qt3 tread. As the road continues to climb, bedrock is exposed in the valley wall.
- 1.6 Cross Christmas Creek. Like the Snahapish River, alluvium from the Hoh River spilled into the Clearwater drainage through this valley.
- 2.0 Climb out of the Christmas Creek valley and ascend onto the Qt2 tread.
- 2.8 Continue along a long, flat portion of the Qt2 tread.
- 3.6 Begin descending the Qt2 tread, stay left on the paved road. The Coppermine Bottom Campground can be accessed via the dirt road to your right.
- 4.1 Cross the Snahapish River and stay to the right on the paved road (towards Upper Clearwater Campground).

- 5.0 Here, and at several other places, you will pass exposed gravels of the Qt2 terrace.
- 6.1 Crossing a Qt2 tread.
- 7.5 Cross the Clearwater River at the Upper Clearwater Campground. Qt5 terraces, like the one we observed at the Grouse Bridge, are exposed both upstream and downstream of the bridge on the bank in front of you.
- 8.1 Stay right on the C3100 road. Begin traversing the interfluvium between the Solleks River and Stequaleho Creek, both two major tributaries to the Clearwater River.
- 9.8 Turn left onto the C3140 road. Note that this road is gated by the Washington Department of Natural Resources just past the junction with the C3100 road. Vehicle traffic past this gate is allowed by permission of the Department. To obtain permission and a key to the gate, contact the Olympic region office in Forks (360-374-6131). Foot and bike access is allowed without permission.
- 11.3 Stay on the main road.
- 13.6 Drop into the Solleks valley bottom.
- 15.2 Cross the Solleks River.
- 15.7 To the south across the old gravel pit is an unobstructed view into the Grouse Creek drainage and the 1997 landslide.
- 16.6 Turn right onto the C3185 road. Cross the Solleks again and begin ascending the ridge on the south side of the river.
- 17.6 Negotiate switchbacks.
- 18.7 Stay to the right, turning onto the C3100 road.
- 19.1 Stay to the right (straight on C3100 road).
- 19.3 Park vehicles near the short access roads connected to the main dirt road. **STOP 2-1. Grouse Creek Landslide.** The objective here is to illustrate the magnitude of mass wasting and sediment delivery to the channel occurring during the Holocene. Note: Due to road deconstruction, one has to walk approximately 1 km to the headscarp of the landslide on the unmaintained road. On March 19th, 1997, 506,000 m³ of rock and regolith moved off this hillslope and into the Solleks River (Serdar, 1999; Gerstel, 1999). The landslide occurred during the waning phases of a major rain-on-snow flood event that started two days prior on March 17th (the St. Patrick's Day flood). Approximately 200,000 m³ of material was deposited on the upper slopes of the Grouse Creek channel, with the remainder

moving as a debris flow that traveled down Grouse Creek, picking up additional material from side slopes, which were scoured up to 54 m high. When the debris flow reached the Solleks River, it deposited approximately 78,000 m³ of material. Landsliding here may have been exacerbated by both a road and associated logging activity; earlier slide scars and additional landslides cut adjacent hillslopes.

The debris delivered to the Solleks channel temporarily dammed the river and pushed the channel to the north. A plume of coarse sediment worked its way down the Solleks into the Clearwater channel by the summer of 1997. The net effect of such instantaneous, point introductions of sediment was to force the channel to enhance its lateral corrasion as the sediment was temporarily stored in floodplains and in channel bars. Downed trees recruited from floodplains trap the sediment and locally made alluvial fills behind dams of woody debris. The abundance of woody debris dams increased in frequency on the Clearwater River in the reach directly downstream of the Solleks confluence.

The exact role that logging and related anthropogenic activities have played in adjusting the hydraulic geometry of the Clearwater channel remains highly debated. The Grouse Creek slide, and other smaller slides have increased the amount of sediment delivered to the channel. That sediment seems to be mostly sequestered in a low terrace (Qt7) colonized by a stand of alder trees, about 30 years old. If changes in the liberation of sediment from hillslopes helps drive the terrace formation process, we must conclude that natural processes during the Holocene have been of greater magnitude than the effects attributed to anthropogenic processes.

The Grouse Creek slide illustrates the dominant process for eroding the steep landscape of tectonically active landscapes. Current thought is that tectonic uplift and river incision will build topography and relief until the hillslopes all have reached a critical slope of failure (Carson, 1970, 1971; Burbank et al., 1996; Montgomery, 2001). Over long periods of time, the liberation of sediment can be viewed as steady, as long as the rates of uplift and incision are steady. But over shorter time spans, the landsliding process is unsteady and is likely modulated by other driving factors, including hillslope moisture and seismically-induced ground accelerations. If the time scale of landsliding unsteadiness is commensurate with the time scale of the process of terrace genesis, we might be able to discern a climatic or possibly an earthquake-cycle tectonic signal from the resulting terrace stratigraphy.

Return to vehicles and retrace the route all the way back to the Upper Clearwater Campground and then on the paved road back to the Snahapish River bridge.

- 31.1 Turn right directly before the Snahapish River bridge (on the Clearwater-Snahapish Road) and begin driving up the Snahapish valley.

- 35.1 Turn right at the major triangle intersection onto the C2000 road.
- 37.9 Loop around steep tributaries. The Qt2 tread is visible in the clearcuts on the right.
- 39.2 Slow and turn right into dirt road marked W-5 or C2017. Pull forward and park to the left in the opening.
- 39.3 Walk south on the overgrown dirt road leading out to an old clearcut.
OPTIONAL STOP 2-A. Terraces at Kunamakst Creek. This is an overview stop to illustrate the presence of terraces, straths, and their considerable separation from the modern channel in the upper Clearwater drainage.
- Return to vehicles and retrace route out to the triangle intersection with the Clearwater-Snahapish Road.
- 47.5 Turn left onto the Clearwater-Snahapish Road.
- 48.4 Turn left into a well-marked gravel pit. **OPTIONAL STOP 2-B. The Qt2 head of outwash in the Snahapish River valley.** The purpose is to examine the coarse-grained, proximal portion of the Qt2 outwash in a gravel pit adjacent to the Qt2 head of outwash. (Figure 3).
- Return to vehicles and continue south (down) along the Clearwater-Snahapish Road.
- 51.6 Turn right and cross the Snahapish River. Ascend the Qt2 tread and slow for the next stop.
- 52.1 Turn right into the Copper Pit. **STOP 2-2. Qt2 terrace at the Copper Pit and cosmogenic surface dating profile.** The purpose of this stop is to show the sedimentology, stratigraphy, and weathering characteristics of the Qt2 terrace and develop the arguments that the underlying strath is 150 ka, whereas the terrace deposit and tread are correlative to the 60-m coastal terrace. Qt2 is the thickest and most widespread fill terrace in the Clearwater valley. Qt2 terrace deposits are made up of 5 to 40 m of coarse stratified sand and gravel that sit on straths 0 to 20 m above the level of the modern valley bottom (Figures 11, 14). Locally, the fill has buried not only the paleo valley bottom (equivalent to the strath) but also the side slopes of the river valley itself, thus forming a buttress unconformity. Sedimentary structures within the terrace deposits include broad, shallow channel forms exhibiting 0.5 to 2 m-high tabular crossbeds, and smaller-scale trough crossbeds of silty sand. These sedimentary structures are generally consistent with a braided channel form and mimic the features exhibited by glaciofluvial deposits that can be physically traced to heads of outwash in adjacent, glaciated drainages. The terrace alluvium is capped by about 1 to 2 m of thin-bedded sand, locally

laminated silt, and massive silt, which are interpreted as both overbank and loess deposits.

Soil profile development and clast weathering rinds (Figure 15) in the terrace treads allow distinctions between deposits of different age and correlation between upstream and downstream remnants of the terraces. Soil descriptions and terminology follow the U.S. Department of Agriculture Soil Taxonomy (Soil Survey Staff, 1975). For the rind-thickness methods, we follow procedures outlined in Chinn (1981), Knuepfer (1988), McSaveney (1992), and Ricker et al. (1993). Rinds were measured to the nearest 1 mm on clasts of greywacke sandstone that were about 4 to 10 cm in diameter and had well-defined concentric rinds and unweathered cores. Most weathering rind studies sample clasts from the surface of the terrace, but this is not possible in the wet and heavily vegetated Clearwater drainage. Good exposures of terrace treads are only available in gravel-pit highwalls and a few road cuts. Otherwise, the treads are either densely forested with no clasts exposed at the surface, or they are significantly disturbed by logging. We avoided this problem by sampling buried clasts collected from a defined position with the terrace soil profile (Colman and Pierce, 1981, 1986). We expect that clasts buried in the soil profile should weather in the same fashion as those at the surface. The soil profile lies within the upper 3 m of the terrace, and thus is relatively thin compared to the thickness of the overall deposit, which might reach some 30 m or more. Furthermore, clasts at the surface and in the soil profile are subjected to similar wet-dry cycles, associated with infiltration of precipitation and fluctuations of the water table.

Sampling was done in high-wall gravel pits, which provide large cross sections, tens of meters in length, of the terrace treads. These exposures show that the soil profiles have been intensely bioturbated down to a depth of at least a meter, and in some cases more, including most of the B horizon of the soil profile. Clasts were collected from the base of the B horizon, where they generally preserve their original depositional fabric, indicating minimal bioturbation. The terrace tread commonly has a fine-grained cap composed of fluvial or eolian sediment. Field and airphoto observations show that soil drainage is poor in areas where this fine-grained cap is thick. In our sampling, we selected areas that were well drained (i.e. minimal fine-grained cap), in order to avoid the influence of variable soil drainage on the degree of clast weathering.

Qt2 deposits have well-developed brownish-red polygenetic soils. Rind-thickness modes are between 9 and 12 mm (Figure 15), and the oxidation depth is about 10 m in coarse sand and gravel. There are 4 distinct treads associated with the Qt2 fill, especially in the region surrounding the Snahapish-Clearwater confluence. The treads are named Qt2a through Qt2d, in order of decreasing elevation and age of the tread. All of these treads show significant postdepositional modification, caused by root bioturbation and colluviation, as well as multiple episodes of loess deposition. Morphology and soil stratigraphy vary on the treads, with well-developed soils on well-drained colluviated slopes and poorly developed loess-

rich soils on eroded interfluvies. In the stable low-relief parts of the tread, the soil consists of a 10 cm-thick A horizon, a local 1 to 10 cm-thick albic horizon, and a 50 to 100 cm-thick B horizon composed of brown (7.5YR) and strong brown (7.5YR) clay loam with moderately thick clay films.

Along the lower Clearwater, the Qt2 strath sits at 15 to 40 m above the modern channel, and its oldest tread, Qt2a, sits at ~60 m above the channel. In the upper Clearwater, the Qt2 strath takes on a steeper gradient, rising to a maximum of 110 m above the modern channel in the uppermost part of the drainage.

The primary tread, Qt2a, marks the constructional top of the original fill unit. The next three treads, Qt2b,c,d, mark a series of unpaired fill-cut terraces that are inset into the primary deposit. These minor inset units are thought to have formed during a series of local events within the river (“complex-response” terraces of Schumm, 1973; Bull, 1991, p. 24 - 25). In contrast, the continuity and paired geometry of the other terrace treads, most notably Qt2a, indicates that they were formed by events that affected the entire drainage.

The Qt2 terrace alluvium represents a time of major Clearwater valley aggradation, when the middle and lower portion of the drainage were hydrologically connected to the Hoh drainage (Figure 3). The Snahapish River, a small underfit stream, marks the former course of outwash fed from moraines in front of alpine glaciers in the Hoh valley. During the penultimate glacial epoch, the head of outwash was at the current location of the divide between the Hoh and Clearwater drainages (Figure 3). The outwash delivered from this moraine created the Qt3 fill, which we will see at the next stop, inset below Qt2.

There is another older head of outwash straddling the middle part of the Clearwater valley (OPTIONAL STOP 2-B) that we think is directly correlative to the Qt2 alluvium and tread here at this stop. Downstream, the Qt2 tread can be traced nearly unbroken to the 60-m coastal terrace, which we have already argued is likely deposited during isotope stage 6 or about 150 ka. So here, we have the upstream projection of that isotope stage 6 fill to its head of outwash in the Snahapish valley. The timing of aggradation must be limited upstream by when the ice margin was stalled in the Snahapish valley pumping out sediment and discharge, and downstream by when sea level was rising to produce the accommodation space leading to the high elevation of the Qt2 tread. This restricts the filling to between 150 to 125 ka. So the strath at the base of Qt2 is taken as 150 ka, and the tread is considered to be younger (Figure 6).

Return to the vehicles, exit the Copper Pit, and continue straight and to the left down to the dirt road that leads to the Coppermine Bottom campground.

52.5

Proceed straight down to the campground. Descend Qt2, cross Crooks Creek slough, and a fill unit inset into the Qt3 tread.

- 53.0 Traverse the Qt3 tread, and turn right.
- 53.5 **LUNCH**, Coppermine Bottom. After lunch, loop through the campground and retrace route out to the Clearwater-Snahapish Road.
- 55.1 Turn left onto the Clearwater-Snahapish Road.
- 59.6 Cross the Grouse Bridge and proceed on the main paved road. After crossing Shale Creek, slow and prepare to turn right.
- 60.6 Turn right into the entrance for an overgrown gravel pit. **STOP 2-3. Qt3 at the Elkhorn Pit.** The purpose of this stop is to show the sedimentology, stratigraphy, and weathering characteristics of the Qt3 terrace and to develop arguments that the underlying strath was buried at 60 ka, and the Qt3 terrace deposit and tread are correlative to the 30-m coastal terrace. The Qt3 terrace alluvium is sedimentologically similar to Qt2. It is everywhere inset into Qt2, buries a strath that is distinctly lower than the strath buried by Qt2, and tends to be, on average, thinner than the Qt2 alluvium (Figures 11 and 14). It has a moderately developed yellow soil profile, rind-thickness modes between 3 and 4 mm (Figure 15), and an oxidation depth of 4 to 5 m, but locally 10 m in coarse alluvium. Postdepositional modification is minimal on the terrace treads, which retain a constructional morphology with well-preserved sandy overbank and silty loess deposits. The loess is more than 1 m near the Snahapish River and near the coast. Soil profiles consist of a 50 to 80 cm thick B horizon composed of yellowish brown (10YR) to brown (10YR-7.5YR) silt loam with numerous thin clay films preserved on soil ped faces. Soil profiles in fine-grained material have strong brown colors (7.5YR) and well-developed soil structure. Qt3 is best preserved below about km 24, where it locally has two treads, designated as Qt3a and Qt3b, with the Qt3b tread sitting about 4 m below the Qt3a tread. In this part of the valley, Qt3 straths maintain a gentle gradient, lying 6 to 10 m above the channel, and treads are 35 m above the channel. Above km 24, Qt3 has only one tread, and the straths take on a steeper gradient, climbing to a maximum height of 70 m above the channel (Figure 14). This gravel-pit outcrop of Qt3 exposes a highwall cut into the Qt3b tread.

The Qt3 tread can be traced upstream through the Snahapish valley to the Lyman Rapids (isotope stage 4, ~ 60 ka) head of outwash in the Hoh valley (Figure 3). Like the Qt2 fill, the time of aggradation of the Qt3 fill was limited upstream to the time when the ice margin was producing discharge and sediment, and downstream to when sea level was rising at the coast. For this reason, we estimate the age of the strath buried by the Qt3 alluvium to be ~ 60 ka and the alluvial itself to be, on the average, several thousands of years younger. There are some data to suggest that the Qt3 fill and Qt3a tread is 48 to 54 ka. A few radiocarbon ages from Lyman Rapids (isotope stage 4) outwash in the Queets and Hoh valleys have finite radiocarbon ages between 47,500±3000 and 54,200+2500/-1900 radiocarbon years before present (Thackray, 1996; 2001) A

landslide exposure north of the town of Clearwater exposes Qt3 alluvium unconformably overlying organic-rich lacustrine beds. The lacustrine beds are radiocarbon dead (> 47,000 radiocarbon years before present), but a log in the Qt3 alluvium returned a finite age of $48,300 \pm 3,300$ radiocarbon years before present (Wegmann, 1999). These ages are at the limit for radiocarbon, but they are stratigraphically consistent with our mapping which places the lower lacustrine beds correlative with the Qt2 fill, and the upper Qt3 alluvium genetically related to stage 4 alpine glaciation.

Return to vehicles and return to the Clearwater-Snahapish Road. Turn left.

- 61.6 Cross Shale Creek. Stay to the right and proceed onto the C1000 road. This road will ascend the Qt3 tread, here about 30 m above the valley bottom.
- 62.9 Ascend the degraded remnants of a Qt2 tread.
- 63.4 Stay right on the major C1000 road. The dirt road leading off to the left is the old approach to the former Goodyear Bridge, an old suspension bridge no longer suitable for vehicle traffic. C1000 continues to follow a Qt3 tread.
- 65.2 Cross Deception Creek and then begin ascending the bedrock ridge north of the Deception Creek drainage.
- 65.6 Find a safe place to park. You may have to take advantage of the C1200-C1000 road intersection 0.5 mile farther up the road. This is where we need to descend the bank down to the Clearwater River. At the river, find a gravel bar and follow it onto the big north-facing meander loop. **STOP 2-4. Crooks Creek terraces.** The objective here is to use the view to illustrate the magnitude of strath separation and resulting river incision rates. The maps and ages of Pleistocene and Holocene terraces will be used to develop models of terrace formation influenced by climatic and tectonic forcings. Visible from this locality, inset below the Pleistocene terraces, are several well preserved Holocene strath terraces (Qt4 through Qt7). These terraces are composed of a basal, coarse grained, 1 to 3 m thick axial-channel sandy gravel facies, which is overlain by a fine grained 1-3 m thick sandy silt overbank facies. The sandy gravel facies locally preserves sedimentary structures consistent with lateral accretion processes, as expected for point bar and transverse bar deposits.

The Holocene terraces are both paired and unpaired, and widely distributed, although some channel reaches are devoid of terraces. In any 500 m reach where the terraces are preserved, we can distinguish three major strath terraces Qt4, Qt5, and Qt6. The underlying straths for these different terraces are clearly at different heights, with differences of at least 2 m (Figures 11). The Holocene terraces are best preserved between valley km 15 and 30, and provide critical information about the lateral extent and morphology of these terrace units (Figure 16). Here the valley bottom has narrowed to 500 m, but the channel maintains an active

meandering pattern. Qt5 tends to equal or exceed the width of the modern valley bottom evident on a 7.5-minute topographic map, whereas Qt6 is wholly confined to (and helps define) the modern valley bottom. Mapping the terraces through this reach clearly demonstrates that the straths have a broad lateral extent. We are able to physically trace a strath and its overlying terrace deposit for hundreds of meters, in some cases of nearly continuous exposure along the river bank. Uniform relative separation between the terrace strath and valley-bottom strath allows us to confidently project between exposures. The deposits in the modern channel are similar to the Holocene terrace deposits. The modern channel contains a mostly continuous mantle of uniform-thickness sandy gravel bars and fine grained overbank silt, sitting atop a broad, laterally continuous, low-relief bedrock strath.

The Crooks Creek exposures show a flight of Holocene terraces Qt4, Qt5, and Qt6 (Figure 16). On the north (far) bank of the river, the alluvium overlying the highest straths (Qt4) has been dated as $8,880 \pm 65$ and $6,985 \pm 60$ radiocarbon years before present. The Qt4 strath is several meters lower at the large south-meander loop, coincident with a Qt4 channel inset into the strath dated at $6,040 \pm 65$ radiocarbon years before present. This degree of strath relief and range in ages is the maximum we observe for a given mapped terrace. The Qt5 strath is exposed on the south bank, straddling the neck of the north meander loop. The alluvium atop the Qt5 strath is dated at $5,410 \pm 50$ radiocarbon years before present. Qt6 underlies the point of the north meander loop and is bracketed by numerous ages (2020 ± 60 to 373 ± 40 radiocarbon years before present) both up- and downstream from the exposures at this stop.

The radiocarbon dates of all Holocene terraces define three broad age groups when plotted on a probability density curve (Figure 17) constructed by the intergration of the probability density distributions for ^{14}C ages corrected to true age (using the OxCal program of Ramsay, 2000). The age groups are defined by prominent breaks at 600 and 1200 years where we have no record of terrace alluvium. From this we infer that Qt4, Qt5, and Qt6 were deposited at 9,000 to 11,000 ybp, 4,000 to 8,000 ybp, and 0 to 3,000 ybp, respectively. Our stratigraphic assignments are consistent with the age data. In other words, at no place along the river does a terrace stratigraphically seem to be Qt6, but has an age in the Qt5 range. Furthermore, stratigraphically older terraces yield the older ^{14}C ages. As a result, the elevation of the strath alone seems sufficient to judge the relative age and correlation of the terraces, even though the alluvium mantling a given strath may have a broad age range.

Bedrock incision is measured using two methods. The strath height above the channel was measured using an altimeter or measuring tape to obtain relative vertical elevation, which has a cited two standard error (2SE) precision of 1 m. Some straths greater than 20 m above the modern channel were measured by positioning the modern channel and the strath relative to the 12 m contours on

U.S. Geological Survey 7.5 minute topographic maps. We used a relative standard error (RSE) of 5.5% to represent the uncertainty for all height measurements.

Estimated incision rates are affected by errors in both height and age. The approximate uncertainties (2SE) for the age of strath burial are: $Qt_2 = 140 \pm 20$ ka (± 14 percent) and $Qt_3 = 65 \pm 10$ ka (± 15 percent). Incision measurements and incision rates for the Qt_2 and Qt_3 straths are shown in Figures 18 and 19, respectively. The error bars for the incision rates include only height errors, because the uncertainty in strath age is common to all incision rates from the same strath. The uncertainties for both height and age give a combined uncertainty of 2 relative standard error of about 18%.

Both Qt_2 and Qt_3 straths show increased incision upstream (Figure 19). Incision rates are remarkably similar for both straths. Smooth curves fit to the data indicate incision rates ranging from 0.1 m/k.y. at the coast to 0.9 m/k.y. in the upper Clearwater valley.

Holocene incision rates are determined from the separation between dated Holocene straths and the valley-bottom strath, which is considered equivalent to the low water level during summer base-flow discharge. This is an appropriate datum from which to measure strath height separation because it helps mark the reach-length average elevation of the valley-bottom strath and avoids measurements affected by local relief in the channel. The incision rate is taken as the amount of incision that has occurred after strath burial (Pazzaglia and Brandon, 2001). Our best estimates for the timing of strath burial are the numeric ages from the overlying terrace deposit, but such ages tend to underestimate the maximum age of the alluvial fill. Thus, our estimates may be biased toward faster rates. Estimated errors include the uncertainties for the ^{14}C age, the elevation of the summer base-flow water level, and the measurement of strath height (including uncertainties with the physical measurement of the height and the natural variation in the outcrop). The relative uncertainty for incision rate is greatest for the youngest terrace (Qt_6) and decreases with increasing terrace age and separation above the channel. Incision rates range from 0.05 – 1 mm/yr in the lower third of the drainage to 1 – 2 mm/yr in the medial portions, to 2 – 3 mm/yr in the upper third (Figure 20). Although similar in pattern to the incision documented for Pleistocene terraces (Pazzaglia and Brandon, 2001), Holocene incision rates exceed Pleistocene rates by a factor of 3 to 2.

Field Trip End. Retrace route out to the paved Clearwater Road.

Concluding Remarks

Our study uses fluvial geomorphology to measure incision and rock uplift across the Olympic sector of the Cascadia Subduction Zone. A well-preserved terrace stratigraphy in an unglaciated drainage, together with reasonable age control for the terrace deposits, allow us to use the valley profile of the Clearwater as a crude geodetic datum. As such, we are able to quantify the effects

of both the short-term earthquake cycle and permanent wedge deformation driving uplift across the interior of the Olympic Peninsula. We summarize 7 major conclusions here.

- (1) Pleistocene terrace sequences in the Olympics seem to be closely tied to the glacial climate cycle through its influence on local climate, sediment supply from adjacent alpine-glaciated drainages, and eustasy. The sequence of terrace-forming events is consistent with the model of Bull (1991), but the timing of these events relative to the eustatic cycle is quite different. Bull (1991) proposed that strath formation occurred during rising sea level and aggradation during falling sea level. In the Olympics, strath formation seems to occur during peak glaciation (when sea level is low), and aggradation during late glacial and interglacial times, when sea level is rising. We suspect that this difference is a local effect, related to the strong influence that local deglaciation has had on sediment supply and the interaction of that enhanced sediment supply with rising sea level during interglacial times.
- (2) Holocene terraces represent local-scale processes of enhanced lateral incision, valley-bottom widening, and the carving of straths accomplished with the aid of the thin alluvial deposits preserved atop the straths. The age-frequency distribution of the terrace deposits overlying a given strath is consistent with this idea, because the distributions are skewed toward the younger extreme of the age range. Valley bottom narrowing and rapid vertical incision into bedrock is accomplished during relatively brief (1,000 yr) intervals between the carving of the major straths.
- (3) We envision the Holocene Clearwater River as being at or near capacity. The alternations in rates of vertical and lateral incision may be linked to temporal variations in the liberation and delivery of hillslope sediment to the Clearwater channel that affect the “at-capacity” condition. Times of increased hillslope sediment flux favor lateral incision, especially if those times coincide with stable, steady discharges, like those envisioned for the valley-bottom-widening cycles described in Meyer et al (1995). Similarly, and following the same analogy, a reduction in the sediment yield, especially in concert with a flashier discharge, would foster valley-bottom narrowing and vertical incision. Hillslope sediment yield is probably strongly influenced by Holocene climate variations, but that climate record remains poorly understood due to a lack of local high resolution proxy records. We appeal to the possibility that seismic shaking could be a viable mechanism for liberating hillslope sediment when slope moisture conditions are favorable for slope failure, or the slopes are primed with a sufficient thickness of regolith. We emphasize that we do not mean to link an individual earthquake to an individual terrace. For instance, large subduction zone earthquakes occur more than 5 times more frequently than major terrace fill events. We note, however, an analogous situation with frequent large fires in the intermontane west, which can occasionally destabilize a hillslope but only when the climate is relatively dry and the precipitation is seasonal (Meyer et al., 1995).
- (4) The upstream divergence of straths in the Clearwater provides strong evidence that uplift is very slow at the coast and increases to a maximum in the center of the range. This conclusion runs counter to a commonly invoked assumption in fluvial geomorphology that long-term uplift rates can be taken as uniform within a single drainage.
- (5) Pleistocene straths of different ages show a similar pattern of incision rates along the Clearwater, ranges from less than 0.1 m/k.y. at the coast to a maximum of 0.9 m/k.y. in the center of the Olympics. These rates correspond closely with the pattern of long-term

erosion rates indicated by apatite fission-track cooling ages. These observations indicate that, at long time scales (10 to 100 k.y), the average form of the landscape remains close to steady state. This also implies that during each phase of strath cutting, the Clearwater valley profile is able to return to the same steady-state form. Thus, bedrock incision rates seem to be a reasonable proxy for rock uplift rates in the Olympics.

- (6) The profile of incision and erosion rates across the Olympics indicates a close balance between the accretionary and erosional fluxes moving in and out of the wedge. This result supports the hypothesis of Brandon et al. (1998) that the Olympic sector of the Cascadia wedge is close to a flux steady state, but note that this conclusion does not require the topography to be steady as well.
- (7) A buried sea cliff, probably formed at 122 ka, provides evidence of horizontal motion of rock relative to the modern shoreline. The rate of motion is 3.7 m/k.y. to the northeast, which is close to the 3 m/k.y. horizontal material velocity predicted for a frontally accreting steady-state wedge. If this interpretation is correct, then it implies that the shoreline has taken on a steady state configuration with each highstand. As a result, we can view the northeast translation of the Sangamon sea cliff as recording northeast directed shortening across the Olympic uplift. These results are consistent with a kinematic model in which long-term horizontal velocity may account for 20 to 35 percent of the geodetically measured horizontal velocity across the Olympics (Pazzaglia and Brandon, 2001). The remaining 65 to 80% is presumably elastic deformation.

ACKNOWLEDGMENTS

The authors would like to acknowledge long-standing working relationships with geoscientists that have worked with us, supported us, and inspired discussion on the topics presented in this paper. These include, but are not limited to Glenn Thackray, Bill Lingley, Wendy Gerstel, Sean Willett, Joe Vance, Tony Garcia, John Garver, Mary Roden-Tice, and Brian Atwater. We thank the Quinault Nation, State of Washington, Olympic National Park, and Rayonier Inc for access to their respective lands. Research supported by NSF-EAR-9302661, 9736748, and 8707442.

REFERENCES

- Abbe and Montgomery, 1996a, Large woody debris jams, channel hydraulics and habitat formation in large rivers: *Regulated Rivers: Research and Management*, v. 12, p. 201-221.
- Abbe, T. B. and Montgomery, D. R., 1996b, Floodplain and terrace formation in forested landscapes old wood [abstract]: *Geological Society of America, Abstracts with Programs*, v. 28, n. 5, p. 41.
- Adams, J., 1984, Active deformation of the Pacific Northwest continental margin: *Tectonics*, v. 3, p. 449-472.
- Armentrout, J. M., 1981, Correlation and ages of Cenozoic chronostratigraphic units in Oregon and Washington, *in* Armentrout, J. M., editor, *Pacific Northwest Cenozoic biostratigraphy: Geological Society of America Special Paper 184*, p. 137-148.
- Atwater, B. F., 1987, Evidence for great Holocene earthquakes along the outer coast of Washington State: *Science*, v. 236, p. 942-944.

- Atwater, B., 1996, Coastal evidence for great earthquakes in western Washington, *in* Rogers, A. M., Walsh, T. J., Kockelman, W. J., and Priest, G. R., editors, Assessing earthquake hazards and reducing risk in the Pacific Northwest; Volume 1.: U. S. Geological Survey Professional Paper 1560: Reston, VA, United States, U. S. Geological Survey, p. 77-90.
- Atwater, B. F., Stuiver, M., and Yamaguchi, D. K., 1991, Radiocarbon test of earthquake magnitude at the Cascadia subduction zone: *Nature*, v. 353, p. 156-158.
- Beaumont, C., Ellis, S., and Pfiffner, A., 1999, Dynamics of subduction-accretion at convergent margins: Short-term modes, long-term deformation, and tectonic implications: *Journal of Geophysical Research*, v. 104, p. 17,573-17,602.
- Bigelow, P. K., 1987, The petrology, stratigraphy and drainage history of the Montesano Formation, southwestern Washington and Southern Olympic Peninsula [M.S. Thesis]: Bellingham, Washington, Western Washington University, 263 p.
- Bockheim, J. G., Kelsey, H. M., and Marshall, J. G., III., 1992, Soil development, relative dating, and correlation of late Quaternary marine terraces in southwestern Oregon: *Quaternary Research*, v. 37, p. 60-74.
- Brandon, M. T., 1996, Probability density plots for fission-track grain age distributions: *Radiation Measurements*, v. 26, p. 663-676.
- Brandon, M. T., and Calderwood, A. R., 1990, High-pressure metamorphism and uplift of the Olympic subduction complex: *Geology*, v. 18, p. 1252-1255.
- Brandon, M. T., and Vance, J. A., 1992, Tectonic evolution of the Cenozoic Olympic subduction complex, Washington State, as deduced from fission track ages for detrital zircons: *American Journal of Science*, v. 292, p. 565-636.
- Brandon, M. T., Roden-Tice, M. K., and Garver, J. I., 1998, Late Cenozoic exhumation of the Cascadia accretionary wedge in the Olympic Mountains, northwest Washington State: *Geological Society of America Bulletin*, v. 110, p. 985-1009.
- Bull, W. B., 1990, Stream-terrace genesis; implications for soil development: *Geomorphology*, v. 3, p. 351-367.
- Bull, W. B., 1991, *Geomorphic response to climatic change*: Oxford University Press, New York, 326 p.
- Bull, W. B., 1991, *Geomorphic response to climatic change*: Oxford University Press, New York, 326 p.
- Bull, W. B. and Knuepfer, P. L. K., 1987, Adjustments by the Charwell River, New Zealand to uplift and climate changes: *Geomorphology*, v. 1, p. 15-32.
- Burbank, D. W., Leland, J., Fielding, E., Anderson, R. S., Brozovic, N., Reid, M. R., and Duncan, C., 1996, Bedrock incision, rock uplift and threshold hillslopes in the northwestern Himalayas: *Nature*, v. 379, p. 505-510.
- Campbell, K. A. and Nesbitt, E. A., 2000, High resolution architecture and paleoecology of an active margin, storm-flood influenced estuary, Quinault Formation (Pliocene), Washington: *Palaios*, v. 15, n. 6, p. 553-579.
- Chappell, J., Omura, A., Esat, T., McCulloch, M., Pandolfi, J., Ota, Y., and Pillans, B., 1996, Reconciliation of late Quaternary sea levels derived from coral terraces at Huon Peninsula with deep sea oxygen isotope records: *Earth and Planetary Science Letters*, v. 141, p. 227-236.
- Carson, M. A., 1970, The existence of threshold hillslopes in the denudation of the landscape: *Transactions of the Institute of British Geographers*, v. 49, p. 71-95.

- Carson, M. A., 1971, An application of the concept of threshold slopes to the Laramie Mountains, Wyoming: Institute of British Geographers Special Publication N. 3.
- Chinn, T., 1981, Use of rock weathering-rind thickness for Holocene absolute age-dating in New Zealand: *Arctic and Alpine Research*, v. 13, p. 33-45.
- Cleveland, W. S., 1979, Robust locally weighted regression and smoothing scatterplots: *Journal of the American Statistics Association*, v. 74, p. 829-836.
- Cleveland, W. S., 1981, LOWESS: A program for smoothing scatterplots by robust locally weighted regression: *American Statistician*, v. 35, p. 54.
- Clowes, R. M., Brandon, M. T., Green, A. C., Yorath, C. J., Sutherland Brown, A., Kanasewich, E. R., and Spencer, C., 1987, LITHOPROBE - southern Vancouver Island: Cenozoic subduction complex imaged by deep seismic reflections: *Canadian Journal of Earth Sciences*, v. 24, p. 31-51.
- Colman, S. M. and Pierce, K., 1981, Weathering rinds on andesitic and basaltic stones as a Quaternary age indicator, western United States: U.S. Geological Survey Professional Paper 1210, 56 p.
- Colman, S. M. and Pierce, K., 1986, Glacial sequence near McCall, Idaho; weathering rinds, soil development, morphology, and other relative-age criteria: *Quaternary Research*, v. 25, p. 25-42.
- Crosson, R. S., and Owens, T. J., 1987, Slab geometry of the Cascadia subduction zone beneath Washington from earthquake hypocenters and teleseismic converted waves: *Geophysical Research Letters*, v. 14, p. 824-827.
- Dean, R., 1991, Equilibrium beach profiles: Characteristics and Applications: *Journal of Coastal Research*, v. 7, no. 1, p. 53-84.
- DeMets, C., and Dixon, T., 1999, New kinematic models for Pacific-North America motion from 3 Ma to present; I, Evidence for steady motion and biases in the NUVEL-1A model: *Geophysical Research Letters*, v. 26, no. 13, p. 1921-1924.
- DeMets, C., Gordon, R. G., Argus, D. F., and Stein, S., 1990, Current plate motions: *Geophysical Journal International*, v. 101, p. 425-478.
- Dragert, H., 1987, The fall (and rise) of central Vancouver Island: 1930-1985: Geological Survey of Canada Contribution 10586, p.689-697.
- Dragert, H., Hyndman, R. D., Rogers, G. C., and Wang, K., 1994, Current deformation and the width of the seismogenic zone of the northern Cascadia subduction thrust: *Journal of Geophysical Research B*, v. 99, p. 653-668.
- Easterbrook, D. J., 1986, Stratigraphy and chronology of Quaternary deposits of the Puget lowland and Olympic Mountains of Washington and the Cascade Mountains of Washington and Oregon, in Sibrava, V., Bowen, D.Q., and Richmond, G.M., editors, *Quaternary glaciations in the northern hemisphere: Quaternary Science Reviews*, v. 5, p. 145-159.
- Florer, L. E., 1972, Quaternary paleoecology and stratigraphy of the sea cliffs, western Olympic Peninsula, Washington: *Quaternary Research*, v. 2, p. 202-216.
- Fuller, I. C., Macklin, M. G., Lewin, J., Passmore, D. G., and Wintle, A. G., 1998, River response to high-frequency climate oscillations in southern Europe over the past 200 k.y.: *Geology*, v. 26, p. 275-278.
- Gardner, T. W., D. Verdonck, N. M. Pinter, R. Slingerland, K. P. Furlong, T. F. Bullard, and S. G. Wells, 1992, Quaternary uplift astride the aseismic Cocos Ridge, Pacific coast of Costa Rica, *Geological Society of America Bulletin* 104, 219-232.

- Gerstel, W.J., 1999, Deep-seated landslide inventory of the west-central Olympic Peninsula: Washington Division of Geology and Earth Resources, Open File Report 99-2, 36 p.
- Hancock, G. S., Anderson, R. S., Chadwick, O. A., and Finkle, R. C., 1999, Dating fluvial terraces with ^{10}Be and ^{26}Al profiles: Application to the Wind River, Wyoming: *Geomorphology*, v. 27, p. 41-60.
- Holdahl, S. R., Faucher, F., and Dragert, H., 1989, Contemporary vertical crustal motion in the Pacific northwest, *in* Cohen, S. C. and Vanicek, P., editors, Slow deformation and transmission of stress in the earth: American Geophysical Union, Geophysical Monograph 40, International Union of Geodesy and Geophysics Volume 4, p. 17-29.
- Holdahl, S. R., Martin, D.M., and Stoney, W.M. 1987, Methods for combination of water level and leveling measurements to determine vertical crustal motions, *in* Proceedings of Symposium on Height Determination and Recent Crustal Movement in Western Europe: Bonn, Germany, Dumler Verlag, p. 373-388.
- Hyndman, R. D., and Wang, K., 1993, Thermal constraints on the zone of major thrust earthquake failure: the Cascadia subduction zone: *Journal of Geophysical Research*, v. 98, p. 2039-2060.
- Johnson, S. Y., Potter, C. J., and Armentrout, J. M., 1994, Origin and evolution of the Seattle fault and Seattle basin, Washington: *Geology*, v. 22, p. 71-74.
- Kelsey, H. M. and Bockheim, J. G., 1994, Coastal landscape evolution as a function of eustasy and surface uplift rate, Cascadia margin, southern Oregon: *Geological Society of America Bulletin*, v. 106, p. 840-854.
- Kelsey, H. M., 1990, Late Quaternary deformation of marine terraces on the Cascadia subduction zone near Cape Blanco, Oregon: *Tectonics*, v.9, p. 983-1014.
- Knuepfer, P. L. K., 1988, Estimating ages of late Quaternary stream terraces from analysis of weathering rinds and soils: *Geological Society of America Bulletin*, v. 100, p. 1224-1236.
- Maddy, D., 1997, Uplift-driven valley incision and river terrace formation in southern England: *Journal of Quaternary Science*, v. 12, p. 539-545.
- McCrary, P. A., 1996, Tectonic model explaining divergent contraction directions along the Cascadia subduction margin, Washington: *Geology*, v. 24, p. 929-932.
- McCrary, P. A., 1997, Evidence for Quaternary tectonism along the Washington Coast: *Washington Geology*, v. 25, p. 14-19.
- McNeill, L. C., Goldfinger, C., Kulm, L. D., Yeats, R. S., 2000, Tectonics of the Neogene Cascadia forearc drainage; investigations of a deformed late Miocene unconformity: *Geological Society of America Bulletin*, v. 112, p. 1209-1224.
- McNeill, L., Piper, K., Goldfinger, C., Kulm, L., and Yeats, R., 1997, Listric normal faulting on the Cascadia continental margin: *Journal of Geophysical Research B*, v. 102, p. 12,123-12,138.
- McSaveney, M., 1992, A manual of weathering-rind dating for sandstone clasts of the Torlesse Supergroup: *Geological Society of New Zealand Miscellaneous Publication 63A*, 106 p.
- Merritts, D., Vincent, K., and Wohl, E. T., 1994, Long river profiles, tectonism, and eustasy: A guide to interpreting fluvial terraces: *Journal of Geophysical Research*, v. 99, B7, p. 14,031-14,050.
- Meyer, G. A., Wells, S. G., and Jull, A. J. T., 1995, Fire and alluvial chronology in Yellowstone National Park: Climate and intrinsic controls on Holocene geomorphic processes: *Geological Society of America Bulletin*, v. 107, p. 1211-1230.

- Mitchell, C. E., Vincent, P., Weldon R. J., and Richards, M., 1994, Present-day vertical deformation of the Cascadia margin, Pacific Northwest, U.S.A.: *Journal of Geophysical Research B*, v. 99, p. 12,257-12,277.
- Montgomery, D. R., 2001, Slope distributions, threshold hillslopes, and steady-state topography: *American Journal of Science*, v. 301, p. 432-454.
- National Data Buoy Center, 2000, Station Information, U.S. Northwest Region.
<http://seaboard.ndbc.noaa.gov/stuff/northwest/nwstmap.shtml>
- Orange, D. L., 1990, Criteria helpful in recognizing shear-zone and diapiric melanges: Examples from the Hoh accretionary complex, Olympic Peninsula, Washington: *Geological Society of America Bulletin*, v. 102, p. 935-951.
- Ouchi, S., 1985, Response of alluvial rivers to slow active tectonic movements: *Geological Society of America Bulletin*, v. 96, p. 504-515.
- Pazzaglia, F. J. and Brandon, M. T., 2001 A fluvial record of rock uplift and shortening across the Cascadia forearc high: *American Journal of Science*, v. 301, p. 385-431.
- Pazzaglia, F. J. and T. W. Gardner, 1993, Fluvial terraces of the lower Susquehanna River, *Geomorphology*, v. 8, p. 83-113.
- Pazzaglia, F. J., Gardner, T. W., and Merritts, D., 1998, Bedrock fluvial incision and longitudinal profile development over geologic time scales determined by fluvial terraces, *in* Wohl E. and Tinkler, K., editors, *Rivers over rock, Fluvial Processes in Bedrock Channels*: American Geophysical Union, *Geophysical Monograph Series*, 107, p. 207-236.
- Personius, S. F., 1995, Late Quaternary stream incision and uplift in the forearc of the Cascadia subduction zone, western Oregon: *Journal of Geophysical Research B*, v. 100, p. 20,193-20,210.
- Pillans, B., Chappell, J., and Naish, T. R., 1998, A review of the Milankovitch climatic beat: template for Plio-Pleistocene sea-level changes and sequence stratigraphy: *Sedimentary Geology*, v. 122, p. 5-21.
- Ramsay, B., 2000, OxCal v. 3.5: available from <http://www.rlaha.ox.ac.uk/orau/index.htm>.
- Rau, W. W., 1970, Foraminifera, stratigraphy, and paleoecology of the Quinault Formation, Point Grenville-Raft River coastal area, Washington: *Washington Department of Natural Resources Bulletin*, v. 62, 34 p.
- Rau, W. W., and Grocock, G., 1974, Piercement structure outcrops along the Washington coast: Washington, Department of Natural Resources, Division of Mines and Geology, *Information Circular*, v. 51, 7 p.
- Rau, W., 1973, Geology of the Washington coast between Point Grenville and the Hoh River: Washington Department of Natural Resources, *Geology and Earth Resources Division Bulletin* 66, 58 p.
- Rau, W., 1979, Geologic map in the vicinity of the lower Bogachiel and Hoh River valleys and the Washington coast: Department of Natural Resources, *Geology and Earth Resources Division Map GM-24*, scale 1:62,500.
- Rau, W., 1975, Geologic map of the Destruction Island and Taholah quadrangles, Washington: Washington Department of Natural Resources, *Geology and Earth Resources Division Map GM-13*, scale 1:62,500.
- Reilinger, R. and Adams, J., 1982, Geodetic evidence for active landward tilting of the Oregon and Washington Coastal ranges: *Geophysical Research Letters*, v. 9, p. 401-403.

- Ricker, K., Chinn, T., and McSaveney, M., 1993, A late Quaternary moraine sequence dated by rock weathering rinds, Craigieburn Range, New Zealand: *Canadian Journal of Earth Sciences*, v. 30, p. 1861-1869.
- Rogers, G. C., 1988, An assessment of megathrust earthquake potential of the Cascadia subduction zone: *Canadian Journal of Earth Science*, v. 25, p. 844-852.
- Savage, J. C., Lisowski, M., and Prescott, W. H., 1981, Geodetic strain measurements in Washington: *Journal of Geophysical Research B*, v. 86, p. 4929-4940.
- Savage, J. C., Lisowski, M., and Prescott, W. H., 1991, Strain accumulation in western Washington: *Journal of Geophysical Research B*, v. 96, p. 14,493-14,507.
- Schumm, S. A., 1969, River metamorphosis: *Journal of the Hydraulics Division, Proceedings of the American Society of Civil Engineers*, v. 95, p. 255-273.
- Schumm, S. A., 1969, River metamorphosis: *Journal of the Hydraulics Division, Proceedings of the American Society of Civil Engineers*, v. 95, p. 255-273.
- Schumm, S. A., 1973, Geomorphic thresholds and complex response of drainage systems, *in* Morisawa, M., editor, *Fluvial Geomorphology: Proceedings of the 4th Geomorphology Symposium, Publications in Geomorphology*: Binghamton, State University of New York at Binghamton, p. 299-310.
- Schumm, S. A., Dumont, J. F., and Holbrook, J. M., 2000, *Active tectonics and alluvial rivers*: Cambridge, UK, Cambridge University Press, 276 p.
- Schumm, S. A., Mosley, M. P., and Weaver, W. E., 1987, *Experimental Fluvial Geomorphology*: Wiley Interscience, New York, 413 p.
- Serdar, C. F., 1999, Description, analysis and impacts of the Grouse Creek landslide, Jefferson County, Washington, 1997-98: The Evergreen State College Master of Environmental Studies thesis, 171 p.
- Sugai, T., 1993, River terrace development by concurrent fluvial processes and climate change: *Geomorphology*, v. 6, p. 243-252.
- Tabor, R. and Cady, W., 1978b, The structure of the Olympic Mountains, Washington - analysis of a subduction zone: U. S. Geological Survey Professional Paper 1033, 38 p.
- Tabor, R. W. and Cady, W. M., 1978a, *Geologic Map of the Olympic Peninsula*: U.S. Geological Survey Map I-994, 2 sheets, scale 1:125,000.
- Thackray, G. D. and Pazzaglia, F. J., 1994, Quaternary stratigraphy, tectonic geomorphology, and fluvial evolution of the western Olympic Peninsula, Washington, *in* Swanson, D.A., and Haugerud, R.A., editors, *Geologic field trips in the Pacific Northwest, 1994 Geological Society of America Annual Meeting*, Seattle, Washington, p. 2A-1 - 2A-30.
- Thackray, G. D., 1996, *Glaciation and neotectonic deformation on the western Olympic Peninsula, Washington [Ph.D. dissertation]*: Seattle, Washington, University of Washington, 139 p.
- Thackray, G. D., 1998, Convergent-margin deformation of Pleistocene strata on the Olympic coast of Washington, USA, *in* Stewart, I. S. and Vita-Finzi, C., editors, *Coastal Tectonics*: London, Geological Society Special Publication 146, p. 199-211.
- Thackray, G. D., 2001, Extensive Early and Middle Wisconsin glaciation on the western Olympic Peninsula, Washington, and the variability of Pacific moisture delivery to the northwestern United States: *Quaternary Research*, v. 55, p. 257-270.
- Thatcher, W. and Rundel, J. B., 1984, A viscoelastic coupling model for the cyclic deformation due to periodically repeated earthquakes at subduction zones: *Journal of Geophysical Research - B*, v. 89, p. 7631-7640.

- Trenhaile, A., 1997, *Coastal Dynamics and Landforms*: Oxford, Clarendon Press, 366 p.
- Tucker, G. E. and Slingerland, R. L., 1997, Drainage basin response to climate change: *Water Resources Research*, v. 33, p. 2031-2047.
- Wang, K., 1996, Simplified analysis of horizontal stresses in a buttressed forearc sliver at an oblique subduction zone: *Geophysical Research Letters*, v. 23, p. 2021-2024.
- Wegmann, K., 1999, Late Quaternary fluvial and tectonic evolution of the Clearwater River basin, western Olympic Mountains, Washington State [M.S. thesis]: Albuquerque, University of New Mexico, 217 p., 4 plates.
- Weldon, R. J., 1986, Late Cenozoic geology of Cajon Pass; implications for tectonics and sedimentation along the San Andreas fault [Ph.D. dissertation]: Pasadena, California, California Institute of Technology, 400 p.
- Wells, R., Weaver, C., and Blakely, R., Fore-arc migration in Cascadia and its neotectonic significance: *Geology*, v. 26, no. 8, p. 759-762.
- Wells, S. G., Bullard, T. F., Menges, C. M., Drake, P. G., Karas, P. A., Kelson, K. I., Ritter, J. B., and Wesling, J. R., 1988, Regional variations in tectonic geomorphology along a segmented convergent plate boundary, Pacific coast of Costa Rica: *Geomorphology*, v. 1, p. 239-265.
- West, D. O. and McCrumb, D. R., 1988, Coastline uplift in Oregon and Washington and the nature of Cascadia subduction zone tectonics: *Geology*, v. 16, p. 169-172.
- Willett, S. D., Slingerland, R., and Hovius, N., 2001, Uplift, shortening, and steady state topography in active mountain belts: *American Journal of Science*, v. 301, p. 455-485.
- Wolman, M. G. and Miller, J. P., 1960, Magnitude and frequency of forces in geomorphic processes: *Journal of Geology*, v. 68, p. 54-74.

FIGURES

Figure 1. (a) Simplified geologic map of the Cascadia convergent margin, modified from Brandon et al. (1998). HRF = Hurricane Ridge Fault, K = Kalaloch, S = Seattle, O = Mt. Olympus, G = Mt. Garibaldi, B = Mt. Baker, GP = Glacier Peak, R = Mt. Rainier. Beneath the Olympics, the convergence velocity of the Juan de Fuca Plate relative to North America is 36 mm/yr. at an azimuth of 54°, which is nearly orthogonal to the modern subduction zone (option 2 for Juan de Fuca/Pacific in DeMets et al., 1990, and “NA-PA Combined” in DeMets and Dixon, 1999). (b) Major drainages of the Olympic Peninsula. The gray dashed line marks the southern boundary of the last glacial maxima (LGM) of the Cordilleran Ice Sheet. (c) Topographic section across the Olympic Peninsula, parallel to the modern convergence direction (A-A’ in b).

Figure 2. (a) Contour map showing short-term uplift rates (solid contour lines) as determined by geodetic measurements (Savage et al., 1991; Dragert et al., 1994) and long-term erosion rates (shaded contour intervals) as determined by fission-track thermochronology (Brandon et al., 1998, and M. Brandon and M. Roden-Tice, unpublished apatite fission-track ages). Rates are in mm/yr. Areas labeled T_q (diagonal-ruled pattern) along the west coast mark exposures of lower Pliocene shallow marine sediment of the Quinault Formation. The preservation of the Quinault and other adjacent nearshore units indicates slow long-term uplift and erosion along the west coast. (b) Relative motion of major tectonic blocks in the Pacific Northwest calculated from geodetic data with respect to the OC-NA pole. Arrows indicate relative block motion. Onshore

white polygons and black triangles are volcanic deposits and volcanoes respectively. In this interpretation, uplift of the Olympic Mountains is accomplished by transpression between the Oregon Coast Ranges and a proposed Vancouver Island buttress. (Modified from Wells et al., 1998).

Figure 3. (a) Digital shaded-relief image (30 m-resolution DEM) showing the relation of the Clearwater drainage to adjacent drainages and glacial deposits in the western Olympics (glacial data are from Thackray, 1996, 2001; Easterbrook, 1986). BT6, BT4, and WC mark Beach Trail 6, Beach Trail 4, and Whale Creek, where important stratigraphic relationships are exposed along the coast. Profiles B-B', C-C', and D-D' mark cross-valley sections of the Clearwater valley, as presented in Figure 8. (b) Map of the Clearwater drainage. The valley profile is shown as a crooked thin line with tics marking valley kilometers from the mouth of the Queets River at the coast. The straight section (A-A' in Figures 1 and 3) lies along the southeast side of the drainage. Final results were projected into A-A', which parallels the local convergence direction for the Cascadia Subduction Zone.

Figure 4. Schematic section (A-A' in Figure 1) showing the regional-scale structure of the Cascadia Accretionary Wedge (after Brandon et al., 1998).

Figure 5. Field trip route and stops.

Figure 6. Regional stratigraphic correlations for glacial and fluvial deposits in the western Olympic Peninsula and surrounding regions. Note the variable scaling in the time axis. Eustasy curve is from Chappell et al. (1996) for 0 to 140 ka, and Pillans et al. (1998) for 140 to 300 ka. The next column shows deposits associated with advances and retreats of the Cordilleran Ice Sheet in Puget Sound, as synthesized by Easterbrook (1986). The next column shows the stratigraphic record of alpine glaciation in the western Olympics, based on the work of Thackray (1996, 2001) We have excluded his drift unit, called Oxbox Ø and estimated to be 39-37 ka, because it is based solely on an isolated sequence of lake sediment. The final column shows terrace stratigraphy in the Clearwater valley as determined by work presented here.

Figure 7. (a) Photograph of the bedrock and wave-cut unconformity exposed at Beach Trail 4. (b) Annotated photograph of the Quaternary stratigraphy and numeric ages typical of the Browns Point Fm in the vicinity of Beach Trail 4 (from Thackray, 1996).

Figure 8. Digital shaded relief showing the buried Sangamon sea cliff. The cliff shows up as subdued scarp that parallels the coast at a distance 1500 m inland. The feature is visible in the image from about 15 km south to about 5 km north of the Queets River.

Figure 9. Annotated photograph of the Quaternary stratigraphy exposed in the vicinity of Beach Trail 6 (from Thackray, 1996).

Figure 10. A schematic cross section of the modern shoreface and sea cliff and the buried Sangamon sea cliff at the mouth of the Queets River. The section X-X' follows A-A'; it has an azimuth of 54°, parallel to the plate convergence direction.

Figure 11. Composite cross section representing the terrace stratigraphy and general age ranges in the Clearwater drainage. We adopt the convention of naming terraces in order of increasing age where “1” is the oldest (highest) terrace in the landscape and assigning numbers to straths only. In this manner, terrace Qt2 may have more than one tread, which we designate with lower case alpha numeric subscripts (as Qt2a, Qt2b).

Figure 12. Annotated photograph of the Qt5 strath and strath terrace exposed at the Grouse Bridge.

Figure 13. (a) Schematic illustrating the relationship between a terrace (t1, t2), straths, the floodplain, and a valley bottom. (b) The correspondence between the width of the floodplain and the width of the valley bottom strath is corroborated by exposure of the valley bottom strath in tributary channels, shown entering from the right part of the diagram.

Figure 14. Cross-valley profiles of the lower (B-B’), middle (C-C’), and upper (D-D’) parts of the Clearwater valley showing the relationship of the terrace units to the local valley geometry. Locations are shown in Figure 3a.

Figure 15. Thickness distributions for clast weathering rinds for terrace deposits of different stratigraphic age. The probability density curves were calculated using the Gaussian kernel method (Brandon, 1996), with the kernel size set to 2 mm. Qt1-Qrd is from an interfluvium about 180 m elevation on the north divide of Shale Creek. Qt2 is from the Peterson Creek terrace about 130 m elevation. Qt3 is from the Quinault quarry pit about 30 m elevation. Qt6 is from an exposed gravel bar adjacent to the Clearwater River, near the Clearwater Picnic Area, about 2 km south of the town of Clearwater.

Figure 16. Map of river terraces in the medial portion of the Clearwater valley (modified from Wegmann, 1999). Letters following terrace-name designations: a, b, c, d indicate treads that share a common strath; ipc indicates inset paleochannel.

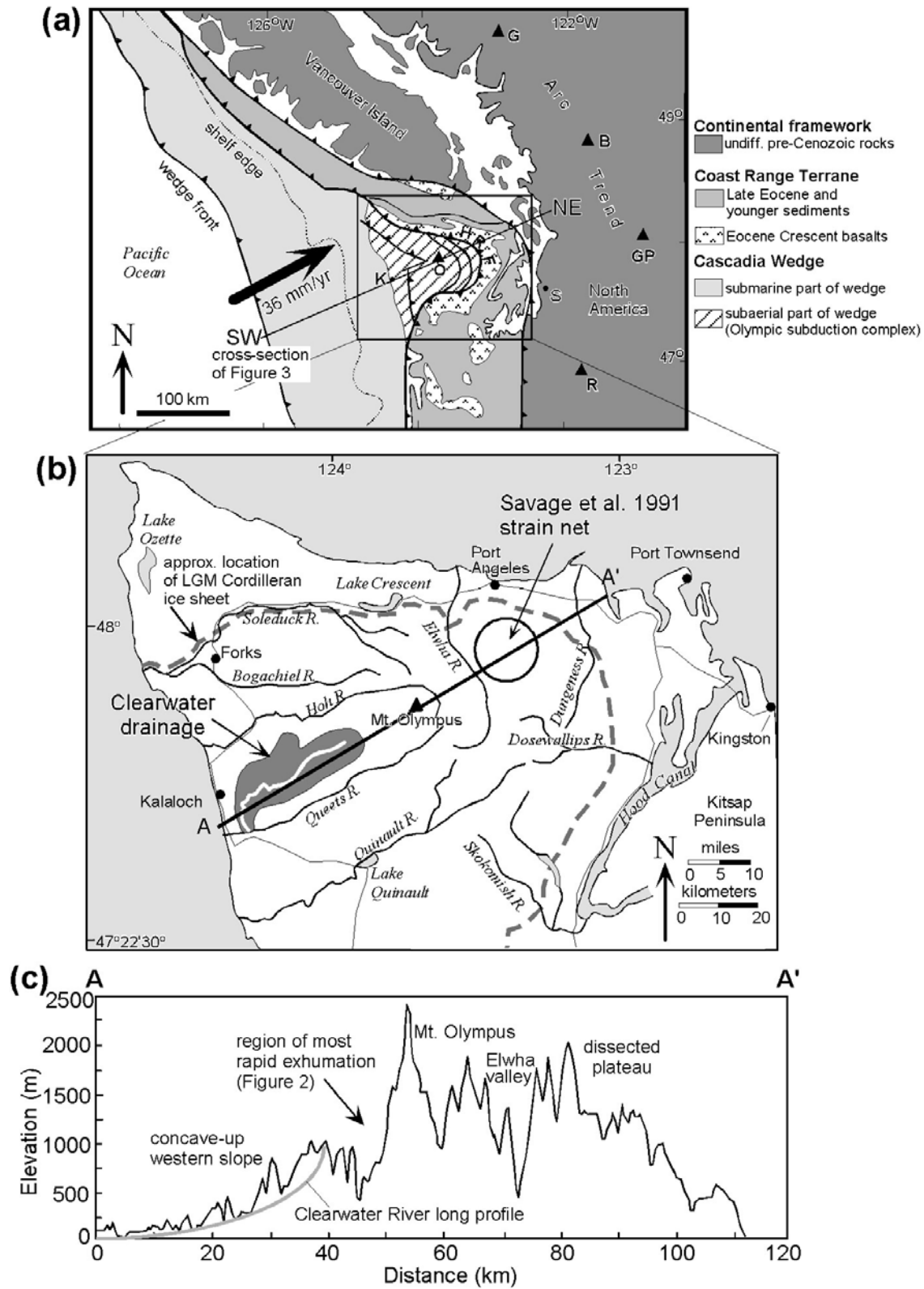
Figure 17. (a) Probability density and frequency plots for 38 radiocarbon dates (Table 1) of the Holocene terraces. The plot was produced by calculating calendar ages, their accompanying 1 sigma errors, and then summing the probabilities using the program OxCal (Ramsay, 2000). Note the brackets beneath the frequency histograms. At the 1σ confidence level, the group of ages between 6000-2000 BC and 1000 BC – AD 2000 statistically coincide with terraces Qt5 and Qt6 respectively.

Figure 18. A long-profile section of the Clearwater valley showing the vertical relationship of mapped terrace deposits (polygons) to the modern Clearwater River (continuous line). Terrace units were projected orthogonally into the valley profile from their mapped positions along the flanks of the Clearwater valley (Figure 3b). The bottom and top of each polygon corresponds to the strath and tread, respectively, for a mapped terrace deposit.

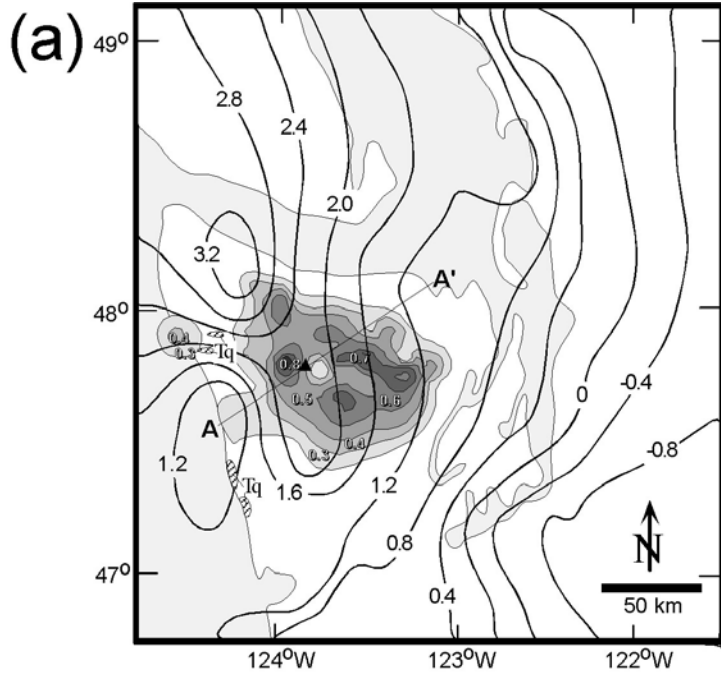
Figure 19. Incision of the (a) Qt2 and (b) Qt3 straths with respect to distance along the valley long profile (see Figure 3b). (c) Incision rates calculated from the Qt2 strath (solid circle) and Qt3 strath (open circle). Note the similarity in the estimated long-term incision rates for these

two different-age straths. In general, incision and incision rates increase in an upstream direction. The small bump in the profiles at about 15 to 25 km suggests some localized uplift, such as a broad fold. Error bars show $\pm 2SE$ uncertainties due to measurement errors for strath height. The thick lines are smoothed from the original data using a locally weighted regression method (Lowess algorithm of Cleveland, 1979, 1981, with the interval parameter set to 0.2).

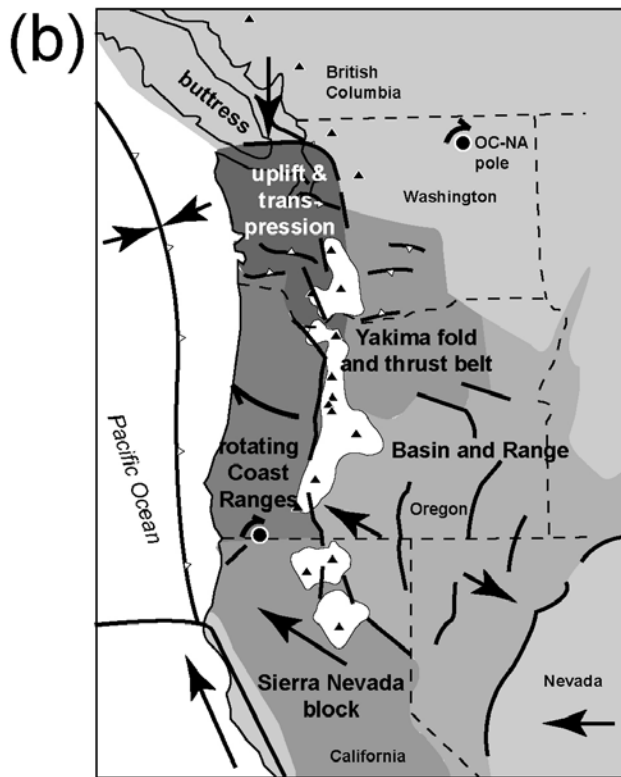
Figure 20. Incision rates (left vertical axis) determined from Holocene terraces (solid black circles) and Pleistocene terraces (gray triangles) plotted with respect to distance along the valley long profile (right vertical axis). Rates reflect calendar ages and error bars on the Holocene data are 1 sigma standard error. Note that the incision rates for both data sets increase upstream.



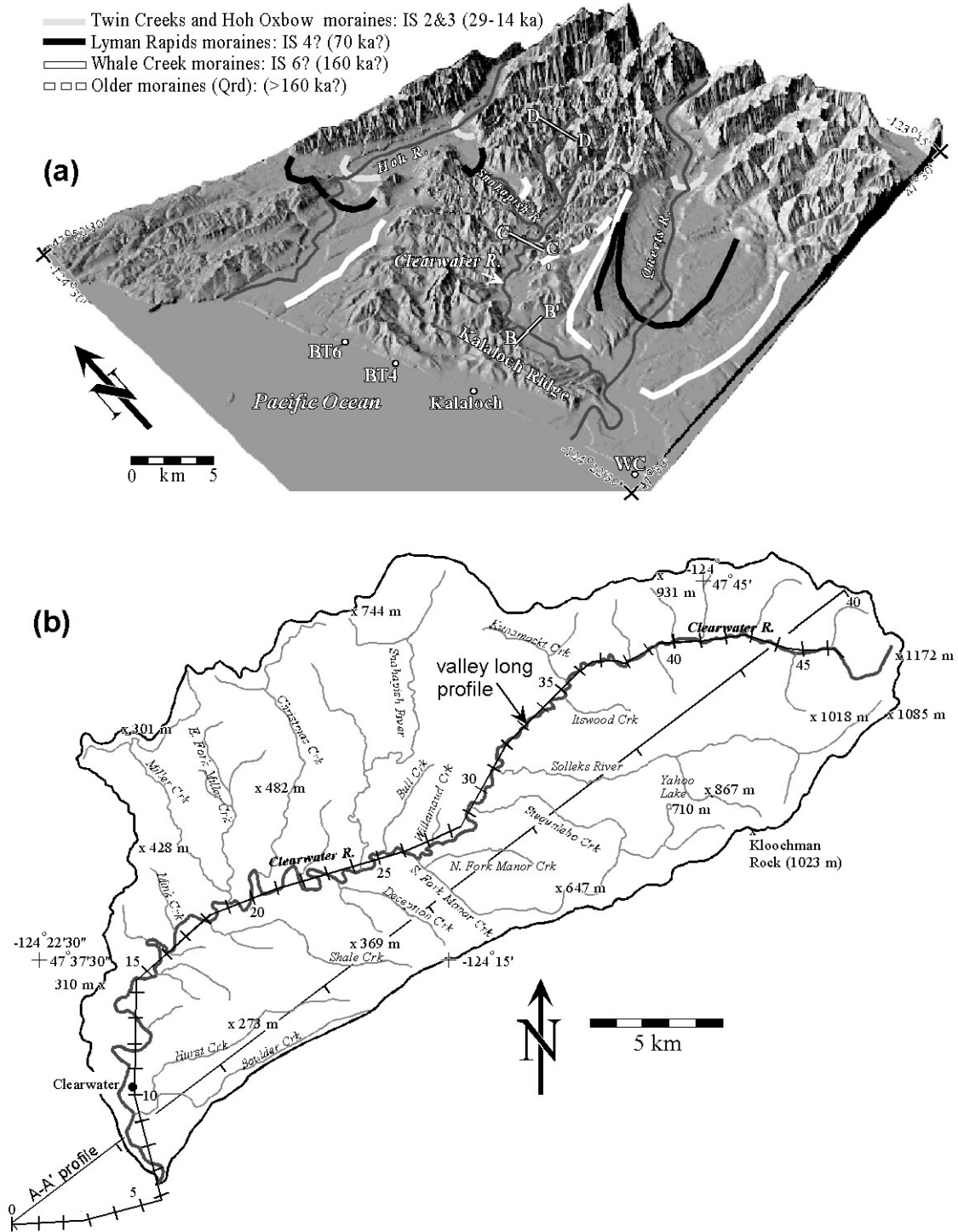
Pazzaglia, Brandon, and Wegmann, 2000, **Figure 1**



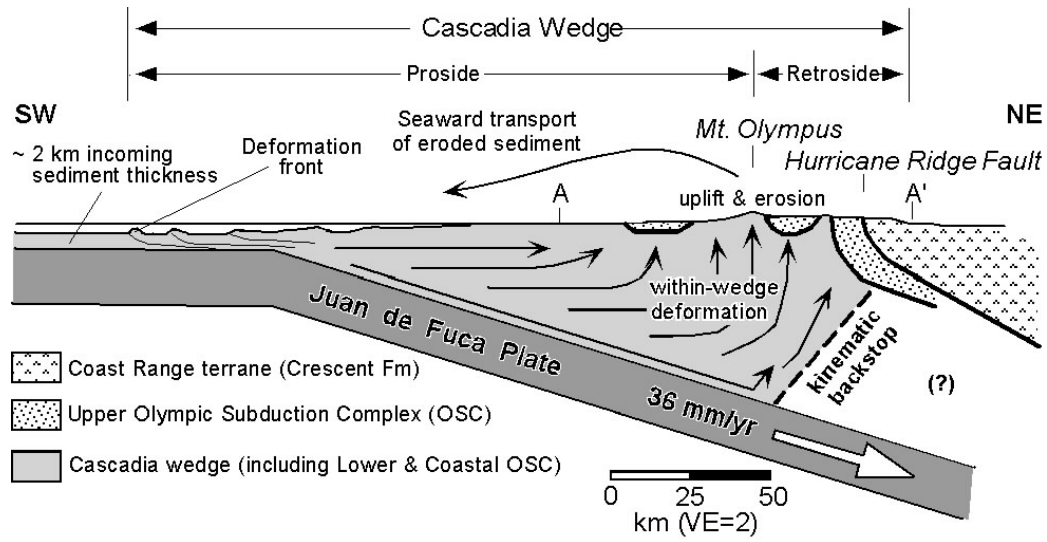
Pazzaglia, Brandon, and Wegmann, 2001 Figure 2a



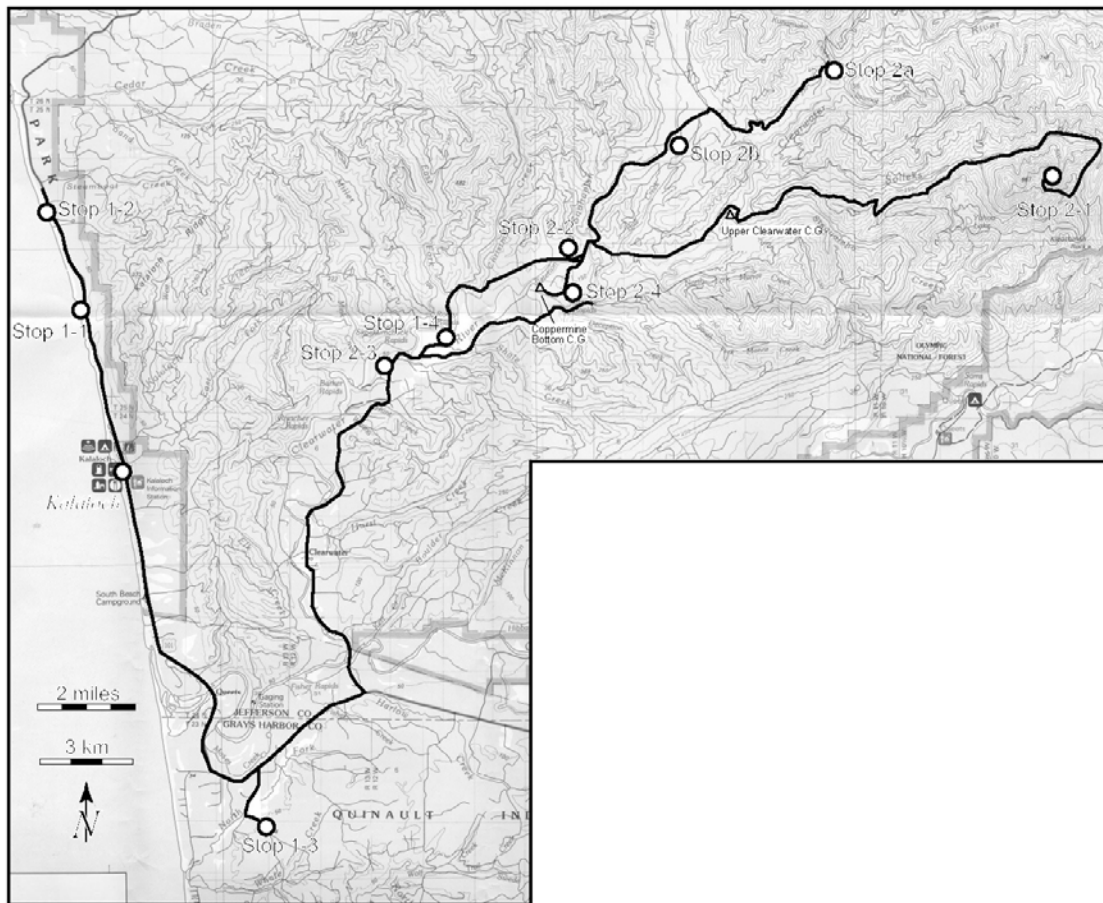
Pazzaglia, Brandon, and Wegmann, 2001 Figure 2b



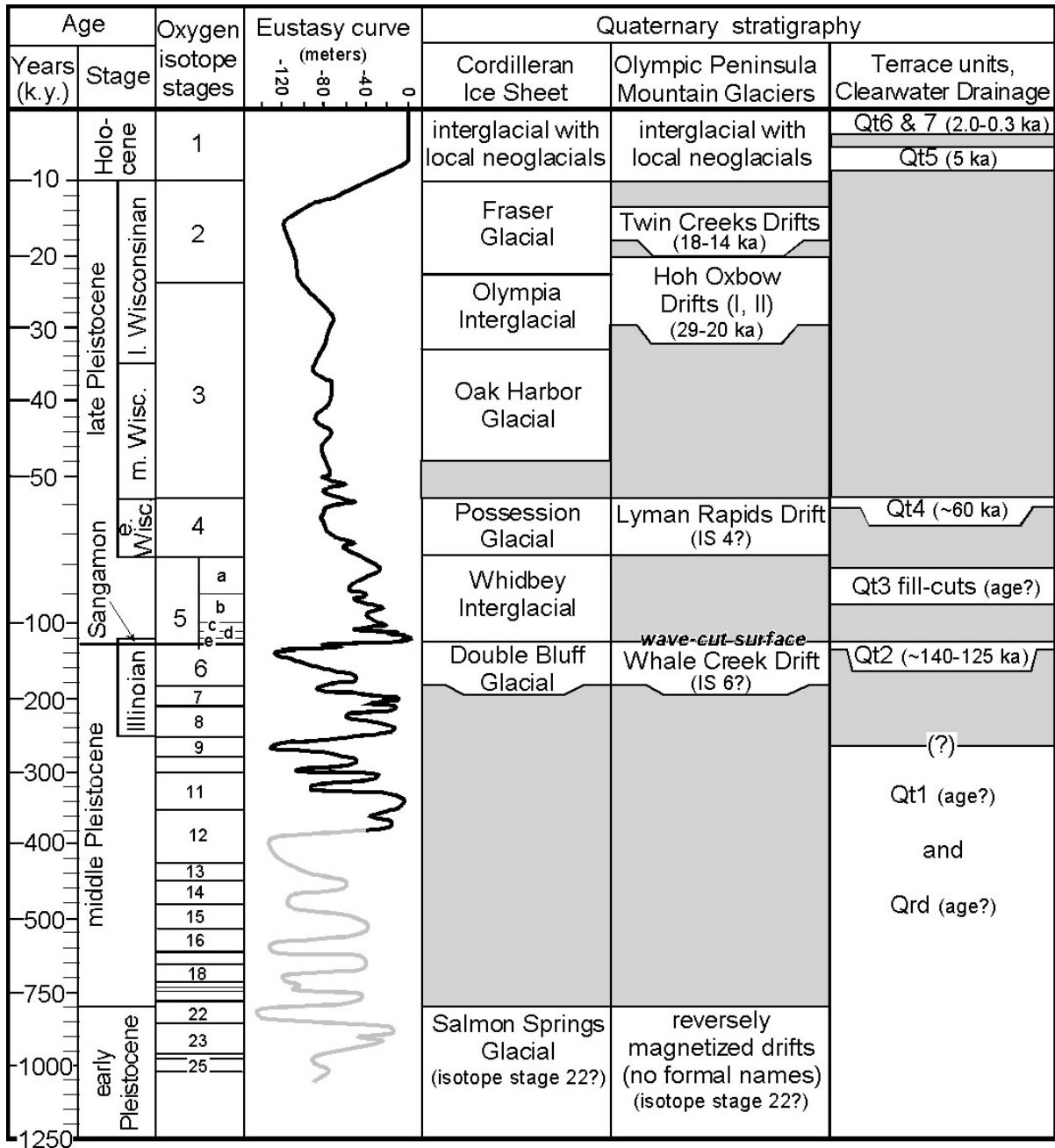
Pazzaglia, Brandon, and Wegmann, 2001 Figure 3



Pazzaglia, Brandon, and Wegmann, 2001, FIGURE 4



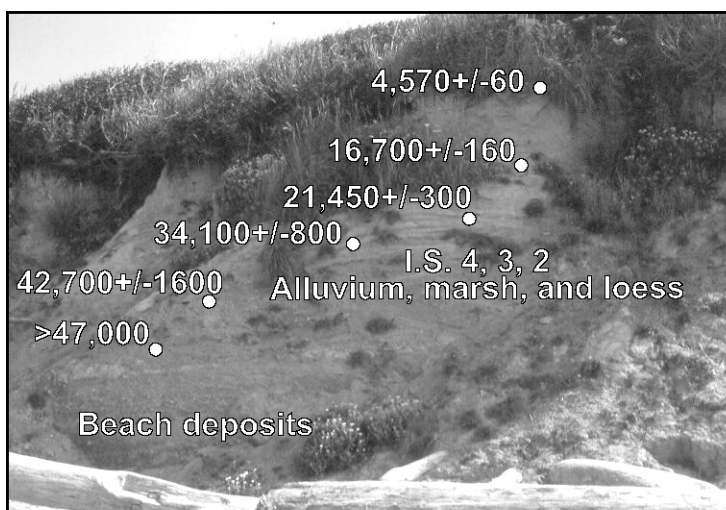
Pazzaglia, Brandon, and Wegmann, 2001 FIGURE 5



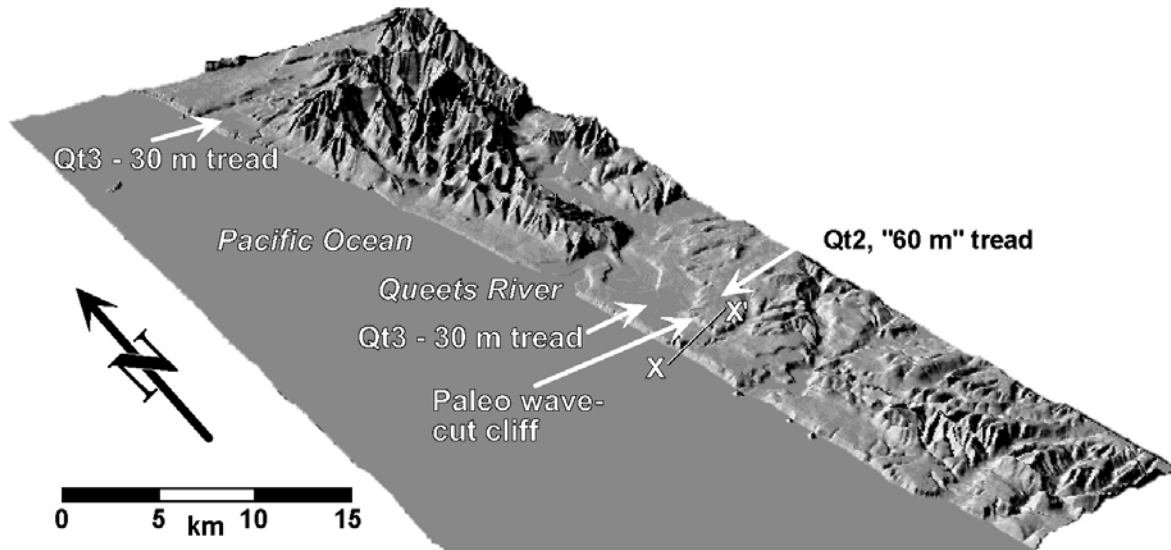
Pazzaglia, Brandon, and Wegmann, 2001, Figure 6



Pazzaglia, Brandon, and Wegmann, 2001 FIGURE 7a



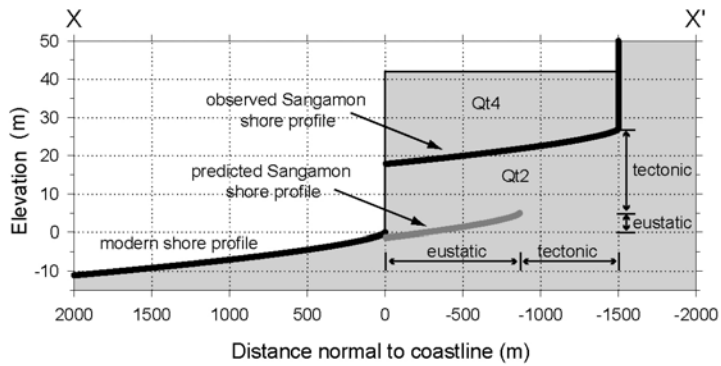
Pazzaglia, Brandon, and Wegmann, 2001 FIGURE 7b



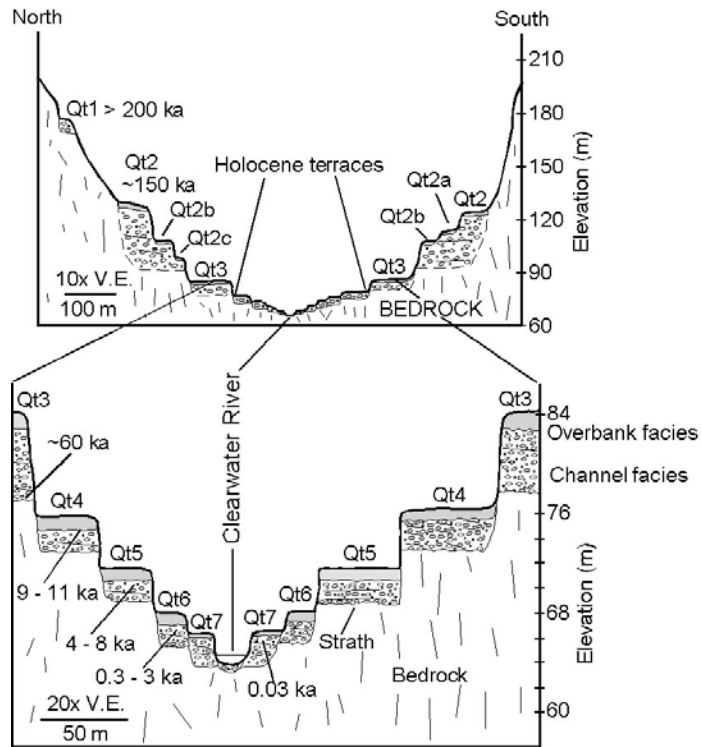
Pazzaglia, Brandon, and Wegmann, 2001 **Figure 8**



Pazzaglia, Brandon, and Wegmann, 2001 **Figure 9**



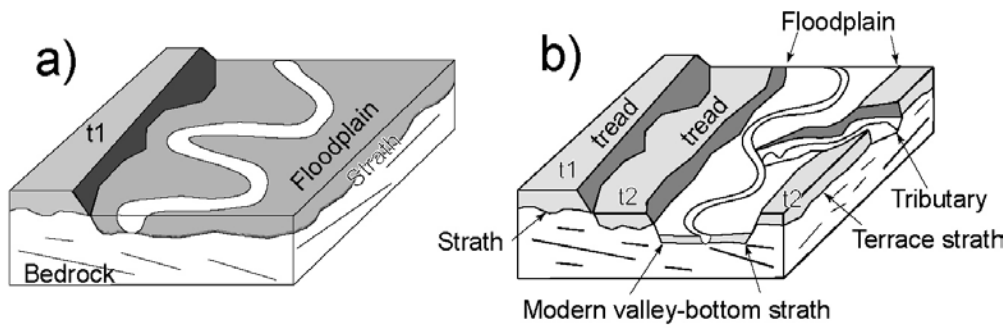
Pazzaglia, Brandon, and Wegmann, **FIGURE 10**



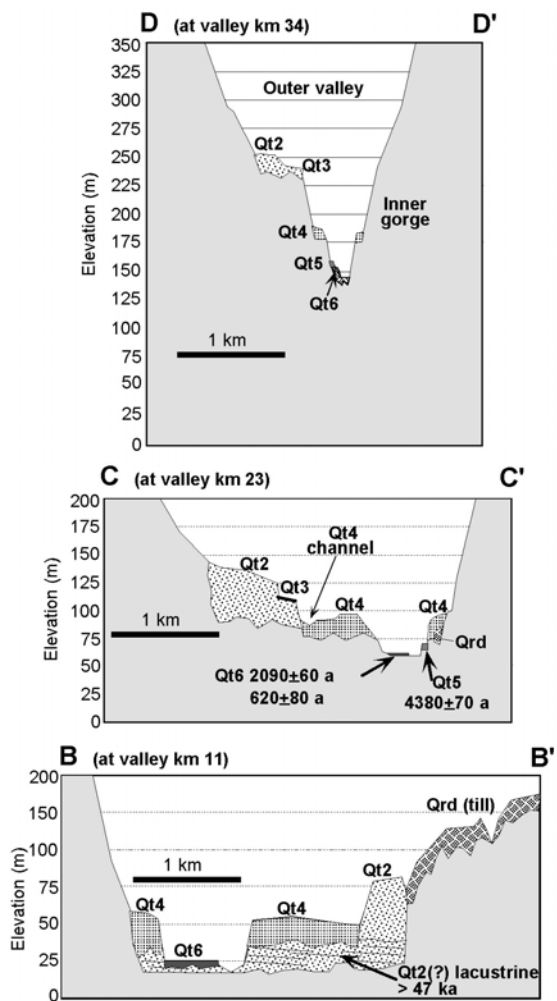
Pazzaglia, Brandon, and Wegmann, 2001, FIGURE 11



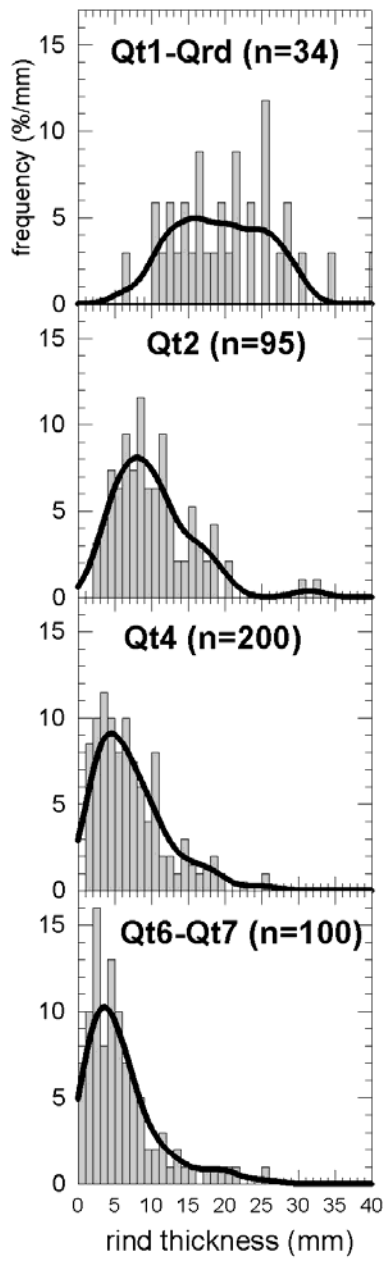
Pazzaglia, Brandon, and Wegmann, 2001, FIGURE 12



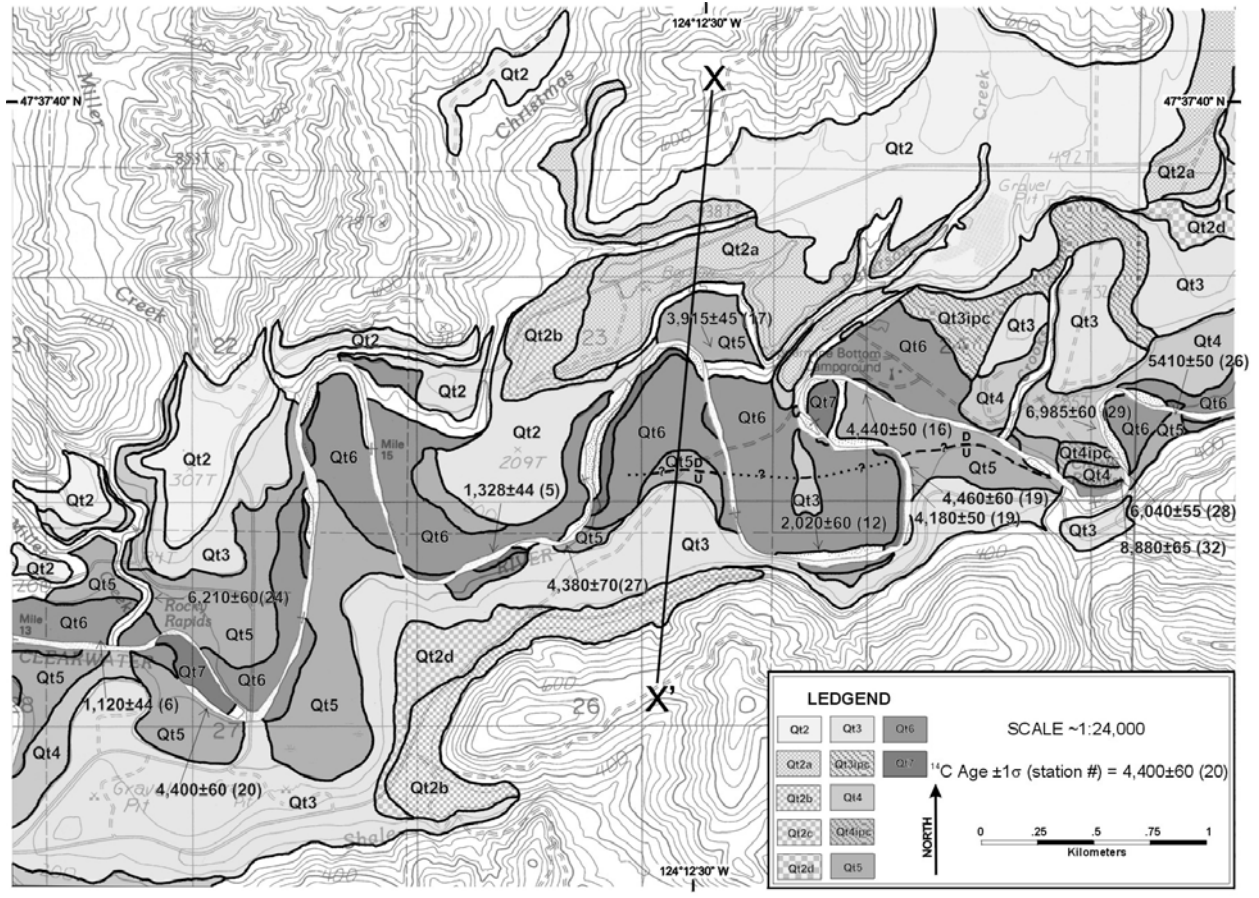
Pazzaglia, Brandon, and Wegmann, 2001, FIGURE 13



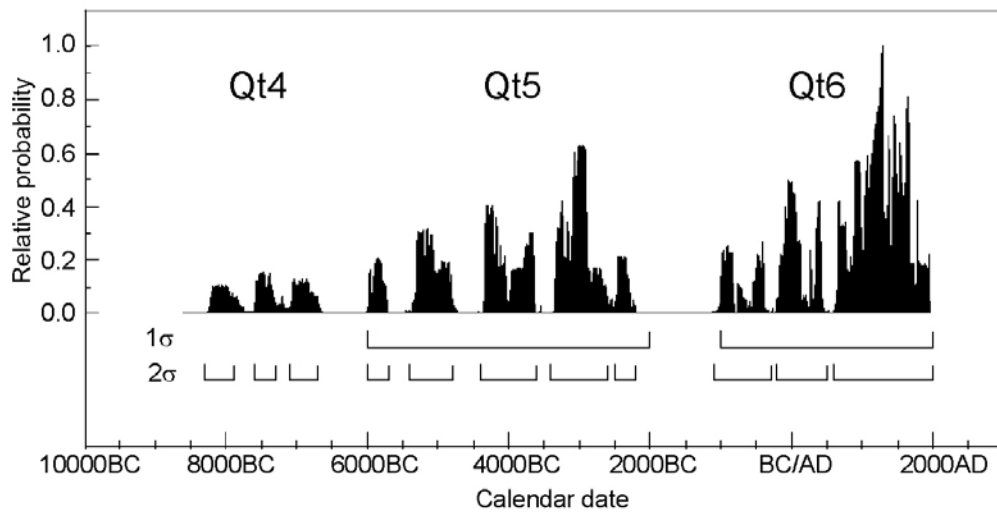
Pazzaglia, Brandon, and Wegmann, 2001, FIGURE 14



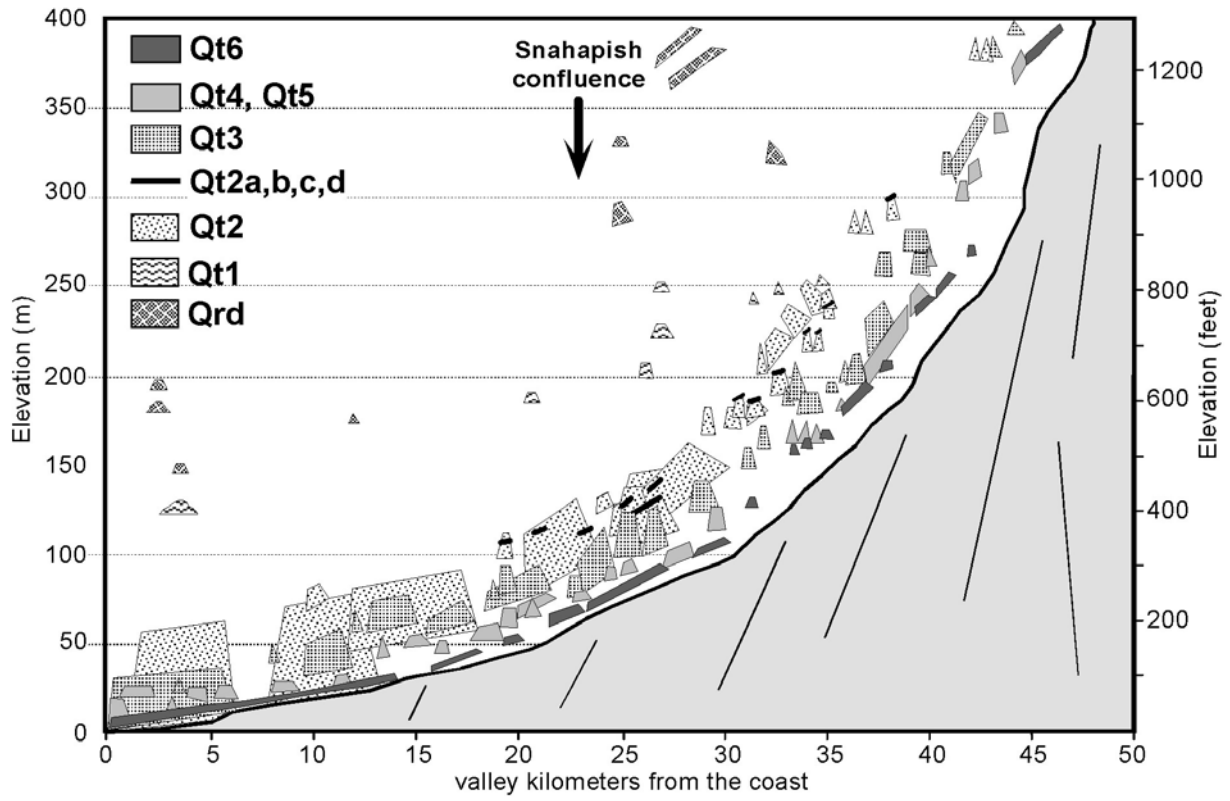
Pazzaglia, Brandon, and Wegmann, 2001 **Figure 15**



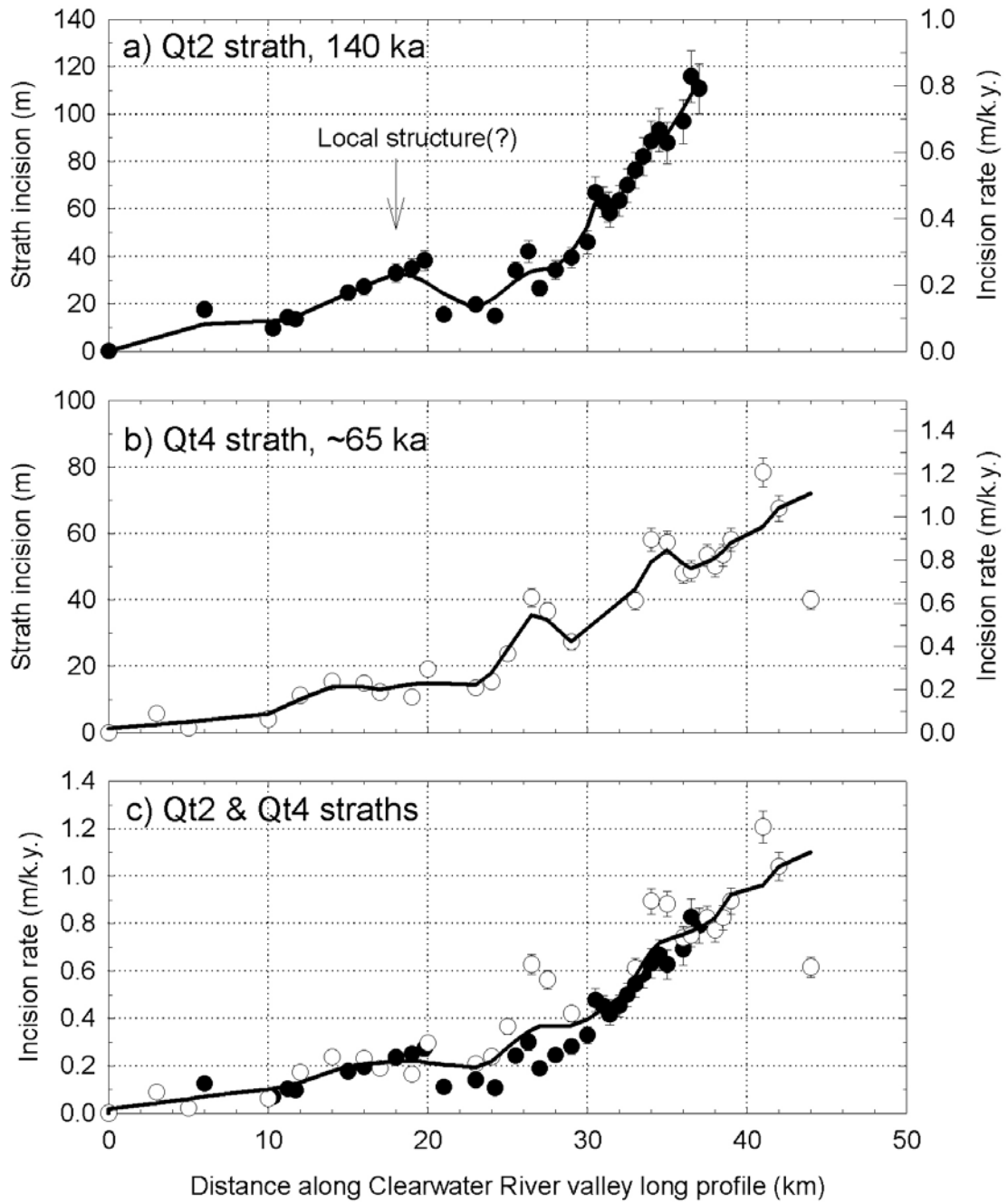
Pazzaglia, Brandon, and Wegmann, 2001, FIGURE 16



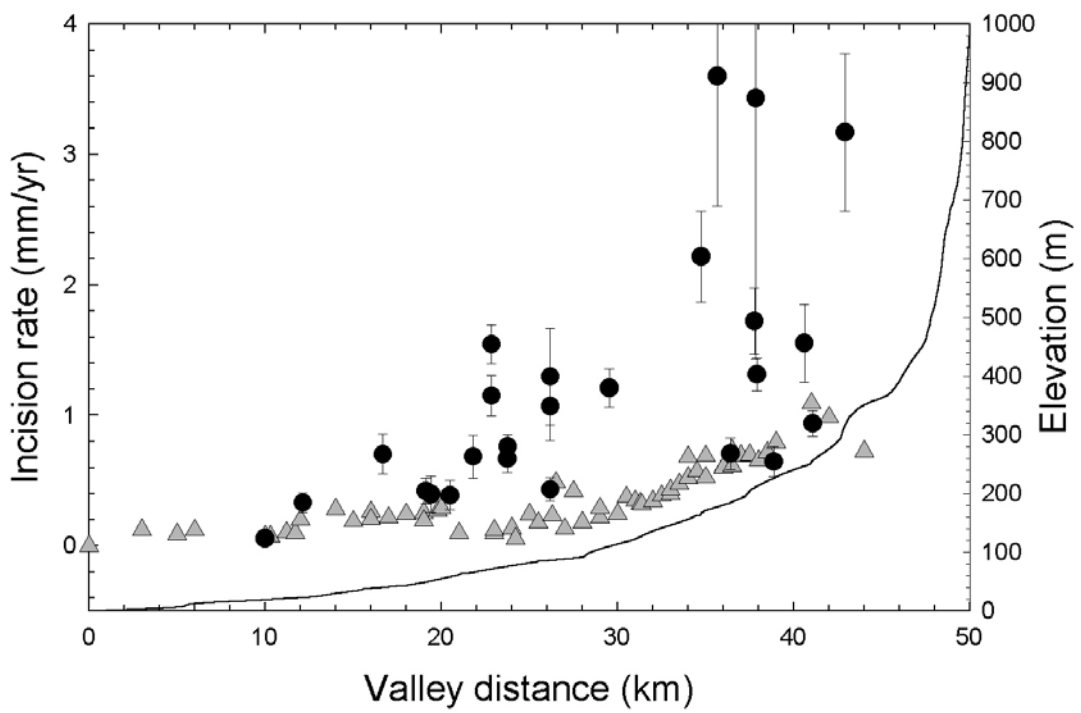
Pazzaglia, Brandon, and Wegmann, 2001, FIGURE 17



Pazzaglia, Brandon, and Wegmann, 2001, **FIGURE 18**



Pazzaglia, Brandon, and Wegmann, 2001 **FIGURE 19**



Pazzaglia, Brandon, and Wegmann, 2001, **FIGURE 20**